European Commission

JRC TECHNICAL REPORTS

Electromagnetic Compatibility (EMC) Evaluation of a Prototype Solar-Charged Electric Race-Car

Radiated and Conducted Emissions based on CISPR 12 and IEC 61851-21-1 automotive EMC Standards and exploratory EMC tests

Pliakostathis, K, Zanni, M, Trentadue, G, Scholz, H. Kluge, H, D, Frankholz, M, Sauer, L, Becker, E, Weckermann, C, Demirci, G, Pautzke, F,

2019

Joint Research Centre

EUR 29991 EN

Contact information
Name: Konstantinos Pliakostathis
Email: konstantinos.pliakostathis@ec.europa.eu

EU Science Hub
https://ec.europa.eu/jrc

JRC118932

EUR 29991 EN

PDF	ISBN 978-92-76-13879-2	ISSN 1831-9424	doi: 10.2760/800123
Print	ISBN 978-92-76-13880-8	ISSN 1018-5593	doi: 10.2760/379632

Luxembourg: Publications Office of the European Union, 2019

How to cite this report: Pliakostathis, K, *et al. Electromagnetic Compatibility (EMC) Evaluation of a Prototype Solar-Charged Electric Race-Car - Radiated and Conducted Emissions based on CISPR 12 and IEC 61851-21-1 automotive EMC Standards and exploratory EMC tests,* Publications Office of the European Union, Luxembourg, 2019, ISBN 978-92-76-13879-2, doi: 10.2760/800123 , JRC118932.

Contents

Foreword 1
Acknowledgements 2
Abstract 3
1 Introduction and Scope 4
2 EMC Standards for Vehicles and On-Board Vehicle Battery Chargers 5
2.1 Maximum allowed limits (radiated and conducted emissions) 5
3 Measurement equipment, laboratory setup and test protocols 7
3.1 VeLA 9 laboratory, receive antennas, instrumentation and test equipment 7
3.2 Vehicle setup 10
3.3 Overview of EMC measurement methods 11
3.4 Measurement challenges 11
4 Results of laboratory measurements 12
4.1 Radiated Emissions (30-1000MHz) 12
4.1.1 Idle State 12
4.1.2 Driving conditions at constant speeds 16
4.2 Conducted emissions (150kHz-30MHz) on AC-Line during charging 20
4.3 Exploratory EMC measurements 22
4.3.1 Radiated Emissions (30-1000MHz) 22
4.3.1.1 Idle State 22
4.3.1.2 Drive State 24
4.3.2 Radiated Emissions (150kHz – 30MHz) during constant speed 26
4.3.3 Time-domain analysis of radiated emissions during dynamic driving conditions 26
4.3.4 Radiation pattern (azimuth scan) around the vehicle during driving/charging 29
4.3.4.1 Charging 29
4.3.4.2 Driving 31
4.4 RF near-field probing (up to 300MHz) 32
5 Conclusions 35
References 36
List of abbreviations and definitions 37
List of figures 38
List of tables 41
Annexes 42
Annex 1. EMC laboratory equipment and instruments 42
Annex 2. EMC test summary 43
Annex 3. Supplementary laboratory illustrations 44
Annex 4. ThyssenKrupp SunRiser vehicle specifications 48

Foreword

This technical report presents and analyses measured results of the electromagnetic compatibility (EMC) profile of a prototype solar-charged electric race-car during driving and charging conditions. Laboratory measurements and setups were based on CISPR 12 and IEC 61851-21-1 automotive EMC standards and on non-legislative exploratory EMC test methodologies, developed by the EC's JRC. Results and main findings of more than 100 different setups managed on V*e*LA 9 validated automotive EMC semi-anechoic chamber, are methodologically extracted from measured data and analysed. The basis of this scientific activity was established to fulfil the objectives of the Interoperability and Electromagnetic Compatibility of Electric Vehicles and their Charging Infrastructure Work Package (WPK INTEC 6311) under the INTEROP-STORE Project (PRJ 208), in collaboration with Bochum University of Applied Sciences, Germany.

Acknowledgements

The Joint Research Centre gratefully acknowledges the scientists of the Solar Car research team, Bochum University of Applied Sciences, Germany, for the provision of the vehicle sample and Andrea Bonamin (AVL, Italy) for his valuable technical support.

Authors

Konstantinos Pliakostathis (JRC of the European Commission)

Marco Zanni (JRC of the European Commission)

Germana Trentadue (JRC of the European Commission)

Harald Scholz (JRC of the European Commission)

Daniel Hans Kluge (Bochum University of Applied Sciences, Germany)

Max Frankholz (Bochum University of Applied Sciences, Germany)

Leon Sauer (Bochum University of Applied Sciences, Germany)

Erik Becker (Bochum University of Applied Sciences, Germany)

Christian Weckermann (Bochum University of Applied Sciences, Germany)

Gökhan Demirci (Bochum University of Applied Sciences, Germany)

Friedbert Pautzke (Bochum University of Applied Sciences, Germany)

Abstract

EMC is an indispensable process throughout the design and manufacturing cycle of any electrical and electronic product. Prior to their launch on the market, these must comply and conform to a series of applicable EMC standards and regulations that aim to protect equipment against EMI. This is more than crucial to automotive EMC as it is associated with the operation of the vehicle's modules and hence the functional safety and reliability of the system against unintentional and intentional EM disturbances. This report presents and analyses the results of EMC laboratory measurements, based on CISPR 12 and IEC 61851-21-1, of a prototype solar-charged electric race-car during driving and charging conditions. The structure of the report is as follows: Section 1 outlines fundamental aspects of EMC and EMI applicable to the electric driven vehicles. Section 2 gives a background of the current automotive EMC regulatory procedures and provides information about the maximum allowed limits. Description of the EMC test facility and the instrumentation used during the measurements is provided on Section 3. Section 4 presents the results of the EMC tests in accordance with the standards, complemented by exploratory test methods, while Section 5 concludes on the main findings of the EMC measurement activity of the prototype vehicle.

1 Introduction and Scope

The ever-increasing penetration rate of new technologies into the automotive market provides unique opportunities in terms of system automation and intelligibility for modern vehicles. The new provisions for autonomous and interconnected vehicles, which are gradually deployed into the production cycle, are assisted by these innovative technologies at component and device level, increasing however too the complexity of these systems. Vehicle safety is of paramount importance to manufacturers and authorities as vehicle systems could be affected by radio frequency interference (RFI) and electromagnetic (EM) disturbances.

Electromagnetic compatibility (EMC) ensures that electronic circuits and software/firmware within digital microprocessors can protect themselves from unwanted RFI and as well minimize their emissions fingerprint, conducted or radiated, on the environment and towards other coexisting wireless or wired systems (Armstrong, 2010).

Automotive EMC has a direct implication on the performance and reliability of vehicle components and elevates the robustness of the electromechanical/electronics systems, which coordinate in many complex ways within modern vehicles and can include on-road driving sensors, collision avoidance radars, GPS navigators, temperature/power sensors, high-speed microcontrollers, safety alarms, on-road driving assistance modules and so on. For these reasons, proper EMC engineering practices must be applied from the design up to the release phase of any vehicle into the market. In addition, automotive EMC protects off-board wireless services, e.g. FM, TV, broadcasting, security communication systems, etc. from being exposed or affected by vehicle EM emissions.

Electric driven vehicles are employing electric motor(s), which is(are) controlled dynamically with power converters and fast switching modules based on pulse-width modulation (PWM) techniques (Mutoh, 2005). As the operating frequency and the switching rate (dV/dt) of these modules increases, so is the EMI contribution by them, either in differential or common mode, with the potential to invade inductively or conductively other vehicle components or radiate on the environment through EM propagation (Skibinski, 1999), (Midya, 2008), (Chen, 2000). Such emissions, can also go beyond 1 GHz (Wisniewski, 2001) and in the worst case scenario, result in the malfunction or failure of near-by co-existing systems exposed to strong EMI. Radiated emissions can also be generated by the recharging units tailored for electric vehicles e.g. (Shall, 2015) and (Pliakostathis-1 *et al*, 2019).

Currently, the type approval procedure for vehicle EMC compliance is defined by Regulation 10 of the UNECE (UNECE, 2014). Part of this regulation defines the EMC test methods for the radiated emissions from the whole vehicle, which are based on CISPR 12 (CISPR 12, 2005). The EMC aspect for the charging infrastructure for electric vehicles (BEVs, PHEVs, etc) is governed by IEC 61851-21-1 IEC (61851-21-1:2017) for *on-board* chargers and IEC 61851-21-2 (IEC 61851-21-2:2018) for *off-board* chargers.

The EMC measurements on this technical report were carried out on a prototype solar-charged race-car inside a validated automotive EMC semi-anechoic chamber for the purposes of assessing its emissions during driving and charging conditions when using an on-board charger (available from the international market). As such, the applied EMC test methodologies were based on the content defined within CISPR 12 and IEC 61851-21-1 for the radiating and conducted emissions, respectively. Furthermore, exploratory work was conducted, beyond the EMC regulatory requirements, to investigate the EM emissions under dynamic driving conditions and different setups by applying novel EMC test methods developed within VeLA 9 of the EC's JRC (described later).

2 EMC Standards for Vehicles and On-Board Vehicle Battery Chargers

Due to the limited time availability of the vehicle, the laboratory measurements were executed, whenever allowed by the EMC standard, by employing the *peak* detector on the EMI receiver (Rohde and Schwarz ESR7), as this provides a quick insight into the measured results and shortens significantly the duration of the tests (Ott, 2009). Furthermore, in comparison to the *average* and *quasi-peak (QP)* detectors, the peak detector provides a greater amount of information of the nature of the electric field during the measurement as it can identify the *actual* level of the emissions and respond instantaneously to shorts bursts and transients generated during a measurement (Williams, 2007). As such, the peak detector was employed during driving (the average detector trace presented on the driving conditions, was included for reference). For the other type of setups (radiated and conducted emissions during charging) the average and quasi-peak detectors were used as typically these types of tests do not require lengthy measurement procedures.

During driving, the vehicle was assessed for its radiated emissions with the test methods and setup as defined within CISPR 12, which in principle require to evaluate the vehicle under a constant speed of 40km/h with the antenna vertically (V-pol) and horizontally (H-pol) polarized, on the left and right side of the vehicle. However, additional exploratory work on the radiated emissions from the vehicle under *dynamic* and *realistic* driving conditions and *different setups* beyond these prescribed within CISPR 12, was conducted both in the time and frequency domain to identify the *actual* emissions. These test methodologies, introduced in (Pliakostathis-1 *et al*, 2019) for vehicle testing and in (Pliakostathis-2 *et al*, 2019) for recharging infrastructure, are outlined on Section 3.3.

The vehicle in consideration was installed with an on-board single-phase AC charger/rectifier for the recharging the high-voltage electric traction DC battery. EMC considerations regarding the radio frequency disturbances from such systems are defined within IEC 61851-21-1, which include, among other tests, assessment of the radiated and conducted emissions during charging.

The limits for each of the aforementioned EMC testing requirements (radiated/conducted) are presented next.

2.1 Maximum allowed limits[1] (radiated and conducted emissions)

For the radiated emissions from the vehicle during driving, the limit lines are defined on Table 1.

Table 1: CISPR 12 peak detector limits for 10m antenna distance for assessing the radiated emissions from the vehicle

Frequency range (MHz)	Distance (m)	Detector type and resolution bandwidth (RBW)	Limit (dBμV/m)
30-75	10	Peak (120 kHz)	54
75-400	10	Peak (120 kHz)	54+15.13 log(f/75), f in MHz
400-1000	10	Peak (120 kHz)	65

For all radiated emissions setups the antenna was placed at 10m away from the vehicle and it was located 3m (1.4m for the active monopole antenna) above the metallic floor of the semi-anechoic chamber.

[1] The incorporation and usage of limit lines within this report is conducted for the purpose of informing the reader on the relative strength of the emissions, conductive or radiated and provide an understanding of the level of these emissions with respect to a reference value i.e. a limit value. As the priority of this report is to share scientific knowledge and disseminate to the EMC community findings from an exploratory work on this vehicle, *no conclusion or link with regard to the compliance or functionality of this vehicle* can be made with the information provided on this report.

For the *conducted* emissions tests, which were carried out for the on-board battery charger connected to a 1-phase AC power line, the limits are defined on Table 4 of IEC 61851-21-1 and are quoted on Table 2:

Table 2: Maximum allowed radio frequency conducted disturbances on AC power lines for on-board vehicle chargers

Frequency range (MHz)	Quasi-peak (dBµV)	Average (dBµV)
0.15 to 0.5	66 Decreasing linearly with logarithm of frequency to 56	56 Decreasing linearly with logarithm of frequency to 46
0.5 to 5	56	46
5 to 30	60	50

IEC 61851-21-1 requires that the vehicle and the on-board charger during charging should be evaluated for the *radiated* emissions, with the limits extracted from Table 7 of the standard and given on Table 3,

Table 3: Maximum allowed vehicle high-frequency radiated disturbances

Frequency range (MHz)	Peak detector (dBµV/m)
30 to 75	32
75 to 400	32 to 43 Increasing linearly with logarithm of frequency
400 to 1000	43

For the assessment of the exploratory radiated emission measurements between 150 kHz and 30 MHz there is (currently) no standard and hence no limit line was indicated on the measured tests,

3 Measurement equipment, laboratory setup and test protocols

This section outlines the laboratory equipment used for carrying out the EMC tests on the vehicle. Annex 1 provides a more detailed description of the test equipment specifications.

3.1 VeLA 9 laboratory, receive antennas, instrumentation and test equipment

A detailed description of the V*e*LA 9 test facility has been provided by (Galassi *et al*, 2015) and (Pliakostathis-2 *et al*, 2019). V*e*LA 9 is an EMC automotive semi-anechoic chamber lined with absorptive material on the walls and it has a volume of 21m x 15.6m x 8m (length x width x height). It is validated for radiated and immunity EMC tests up to 18GHz and due to its size, it allows to conduct measurements at 3m and 10m antenna placement. Inside the SAC, there is a chassis dynamometer roller bench to accommodate vehicles up to 4 tonnes on a 11m in diameter turntable that can make a full rotation whilst the vehicle is driven.

Two different receive antennas were used during the radiated emissions measurements to cover frequencies between 150 kHz and 1 GHz. As stated, the antennas were placed 10m away from the vehicle.

Figure 1: Illustrations of the receive antennas used for the measurement of the radiated emissions (a) Schwarzbeck VULB 9162 Tri-Log antenna, 30-8000 MHz and (b) active monopole E-field antenna ETS Lindgren 3301C, 30 Hz-50 MHz

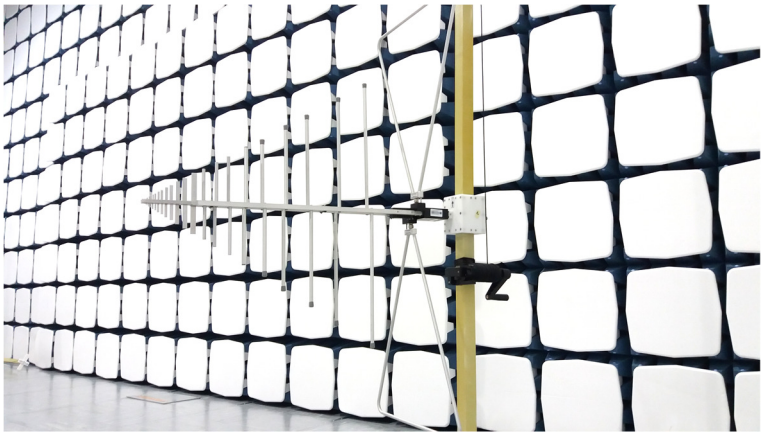

(a)

(b)

The results of the radiated and conducted emissions measurements displayed on the EMI receiver incorporated all the appropriate correction factors, which were the following:

- Antenna factor (radiated emissions)
- Coaxial cable losses (and DC-blocker) between the EMI receiver and the monitoring device (antenna or LISN)
- Attenuation factor for LISN (conducted emissions)

The electric field strength during the *radiated* emissions was calculated from equation

$$E\ (dB\mu V/m) = AF\ (dB/m) + L\ (dB) + R\ (dB\mu V)$$

E is the electric-field strength (dBμV/m) of the EUT i.e. vehicle

AF is the receive antenna factor (dB/m)

L are the losses of the coaxial line/DC-blocker (dB) and

R is the reading of the EMI receiver (dBμV)

while the following equation calculates the value of the RF voltages on the *conducted* emissions,

$$V\ (dB\mu V) = L\ (dB) + R\ (dB\mu V)$$

where,

V is the conducted RF voltage (dBμV)

L are the losses of the transmission line and the attenuation factor (dB) of the LISN

R is the reading of the EMI receiver (dBμV)

Figure 2:The EMI test receiver used for the measurement of the radiated and conducted emissions

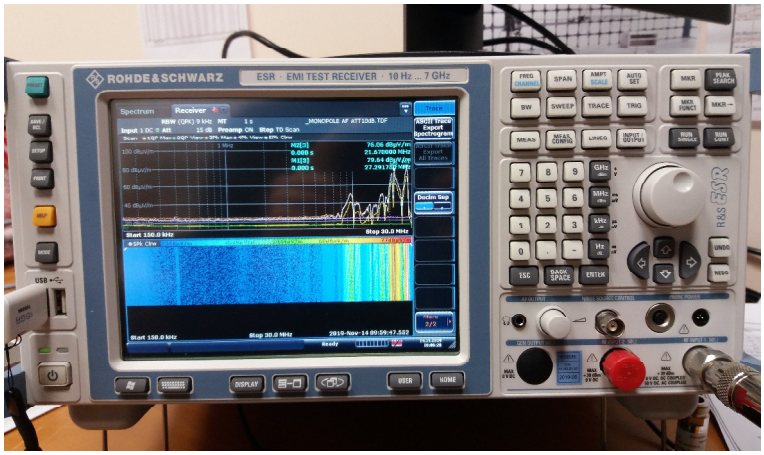

A scanning receiver was employed during the radiated emission measurements with the settings shown on Table 4.

Table 4: Configuration of the scanning receiver during the radiated and conducted emissions (NA: Not Applied)

Frequency range (MHz)	Type of measurement	Peak detector (driving conditions)			Quasi-peak detector (charging conditions)			Average detector (driving and charging conditions)		
		Bandwidth	Step size (maximum)	Dwell time	Bandwidth	Step size (maximum)	Dwell time	Bandwidth	Step size (maximum)	Dwell time
30 to 1000	Radiated	120 kHz	50 kHz	5ms	120 kHz	50 kHz	1s	120 kHz	50 kHz	5ms
150 kHz to 30 MHz	Radiated	9 kHz	5 kHz	50ms	NA	NA	NA	9 kHz	5 kHz	50ms
	Conducted	NA	NA	NA	9 kHz	5 kHz	1s	9 kHz	5 kHz	50ms

For the measurement of the conducted emissions on the AC line, a 50μH/50Ω line impedance stabilization network (LISN) model ENV4200 by Rohde and Schwarz was used, shown on Figure 3

Figure 3: Line Impedance Stabilization Network (LISN) instrument used for the conducted emissions Rohde and Schwarz ENV4200, 150 kHz to 30 MHz, employing a transient limiter for the protection of the EMI receiver

RF near-field scanning was performed to identify the possible physical location of the emissions on the vehicle. This was realized with the use of near-field probes and an oscilloscope to monitor the spectrum of the captured emissions, Figure 4.

Figure 4: Equipment used for near-field RF scanning of the vehicle (a) near-field electric and magnetic field probes by ETS-Lindgren, (b) oscilloscope Wavesurfer 510 by Teledyne LeCroy

(a)

(b)

3.2 Vehicle setup

The vehicle (thyssenKrupp SunRiser, see Annex 4 for specifications) was fixed inside V*e*LA 9 EMC SAC on 11m in diameter turntable, which could perform a full 360 degrees rotation of the chassis dynamometer, with non-conductive straps, Figure 5. In order to replicate as closely as possible realistic on-road conditions during driving, the applicable road load resistance factors were defined within the parameters of the dynamometer system based on the dimensions and weight of this vehicle. In addition, a high-power fan system, appropriate for such EMC tests, was sending the air towards the front of the vehicle during driving.

Figure 5: Antenna and vehicle setup for the measurement of the radiated emissions inside VeLA 9 automotive EMC semi-anechoic chamber

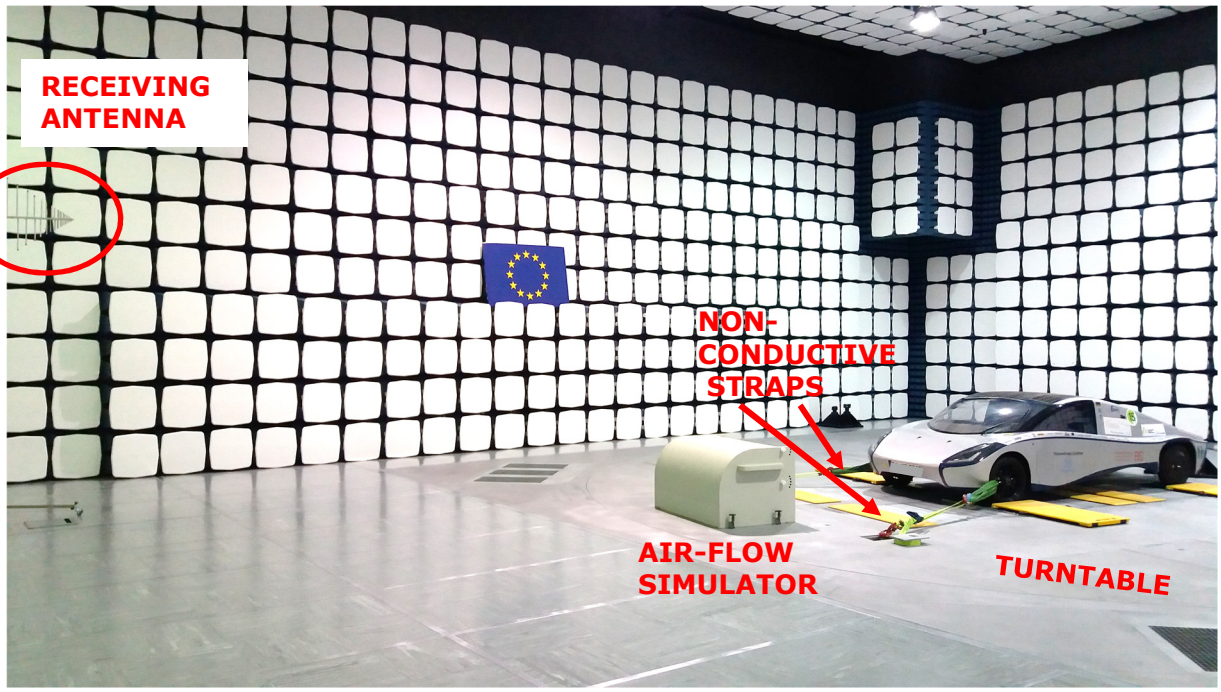

The vehicle's drivetrain consisted of three main components, (i) the battery, (ii) the frequency converters and (iii) the wheel hub motors.

The use of the wheel hub motors allowed to drive the right and the left motor independently. This was relevant when cruise control was active due to a software feature, which reduced the thermal strain and improved power efficiency. This particular feature turned one motor off, when the propulsion power of

one motor was sufficient to drive the car. If the driving force from one motor was not adequate to retain the vehicle speed, the second motor would turn back on.

The temperature of both motors was monitored regularly and the car swapped the driving motor to the motor that had the lowest temperature. Every motor was driven by a frequency converter of the company Tritium. The frequency converter converted the D.C. battery voltage to three-phase A.C. currents and read the sensor data provided by the motor.

The motor was a permanently excited synchronous motor with radial magnetic flux. The motor was located within an aluminium case (aluminium 7075). The casing of the motor was also the wheel itself. The wheel hub motor formed the complete wheel with the rim and the tire and thus it avoided the need of a conventional drivetrain.

The DC battery supplied a voltage between 90V and 151V and a current of maximal 60A per motor. During driving, the battery temperature was elevated up by only 1-2 C°, because it was designed for much higher peak currents.

3.3 Overview of EMC measurement methods

The test protocols and the laboratory setup applied during the measurements for the EMC assessment of the vehicle were based on

1. The test methods described within the applicable EMC standards (CISPR 12, IEC 61851-21-1) and
2. Exploratory test techniques and setups beyond the requirements of the standard to investigate the EM emissions under more realistic driving cycles and test setups.

The detailed methodology and the measurement approach for the definition and execution of these *exploratory* EMC tests on vehicles has been reported in (Pliakostathis-1 *et al*, 2019) and (Pliakostathis-2 *et al*, 2019) and hence only brief description of these techniques will be presented here. The exploratory test methods can be broken down into these distinct steps:

- Investigation of the peak level of EM *around* the vehicle during driving and charging.
- Frequency domain and time domain (fixed at critical EMI frequency) techniques were deployed to associate the nature of vehicle EM emissions with the vehicle's driving state.
- The vehicle radiated emissions test protocols were conducted at different constant speeds and throughout a typical driving cycle to replicate as closely as possible real case scenarios (acceleration deceleration, switching ON/OFF, effect of gearbox, etc.).
- The assessment of the radiated emissions from the vehicle during driving were carried out beyond the CISPR 12 frequency band i.e. 150 kHz to 30 MHz.

3.4 Measurement challenges

During the EMC testing it was observed that the dynamic and electromechanical behaviour of the vehicle was *automatically controlled through software*. For example, when the cruise control was active during driving, the electric power was *dynamically* distributed between the left and right side of the rear motors to optimize, among other parameters, battery efficiency. Considering that these motors were contributing to the EMI emissions this in turn resulted in irregular EM pattern behaviour during some measurements. For this reason, information as to whether the EMC tests during driving were performed either in *manual or cruise control* mode was indicated on the title of the corresponding figures. Furthermore, during some tests, the vehicle received an error indication caused by a malfunction of an on-board temperature sensor.

4 Results of laboratory measurements

The laboratory results of the radiated emissions at standby, during driving conditions and these of the conducted emissions during charging, are presented on this Section. In addition, EMC tests results of exploratory work with the vehicle driven under dynamic and realistic driving conditions, which included E-field monitoring of the acceleration and deceleration phases, and near-field RF scanning, are also presented.

4.1 Radiated Emissions (30-1000MHz)

The first part of this Section presents results of the EMC tests, while the vehicle was idle (i.e. 0km/h) and engaged under different operating conditions which were:

1. Safe state
2. Safe state with parking lights ON
3. Safe state with all lights ON
4. Safe state with break pressed and all lights ON
5. Motor state and idle mode

The second part illustrates the results of EMC measurements taken on the left and right side of the vehicle both for vertical and horizontal polarization, while the vehicle was driven at different constant speeds i.e. 10km/h, 20km/h, 30km/h, 40km/h, 60km/h, 80km/h and 100km/h.

On the following Figures, Trace 1 represents the max-hold of the Peak detector, Trace 2 is the Peak detector noise floor, Trace 3 is the max-hold of the Average detector, Trace 4 is the Average detector noise floor, Trace 5 is the Clear-Write of the Peak detector (used to evaluate field fluctuations during measurements) and Trace 6 is the Clear-Write of the Average detector (used to evaluate field fluctuations during measurements). The red line indicates the CISPR 12 *Peak* detector limit line.

4.1.1 Idle State

Figure 6: Radiated emissions (30-1000MHz), EV ON, 12V system (safe state), V-pol, (a) left, (b) right

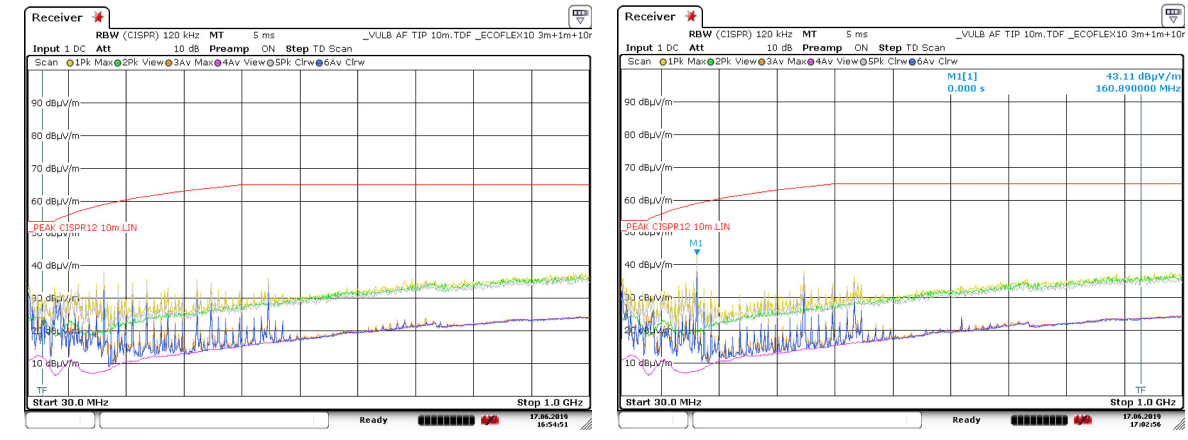

Figure 7: Radiated emissions (30-1000MHz), EV ON, 12V system (safe state, parking light), V-pol (a) left and (b) right, H-pol (c) left and (d) right

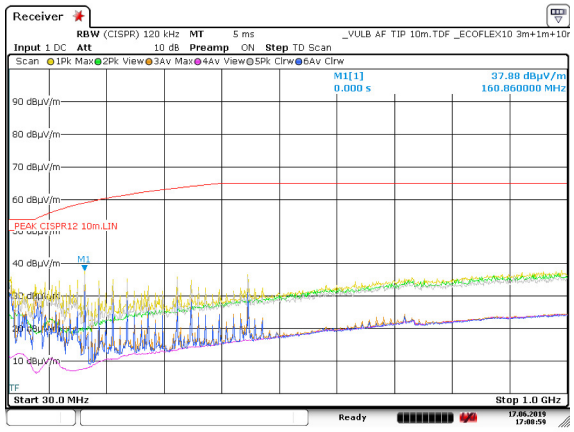

a.

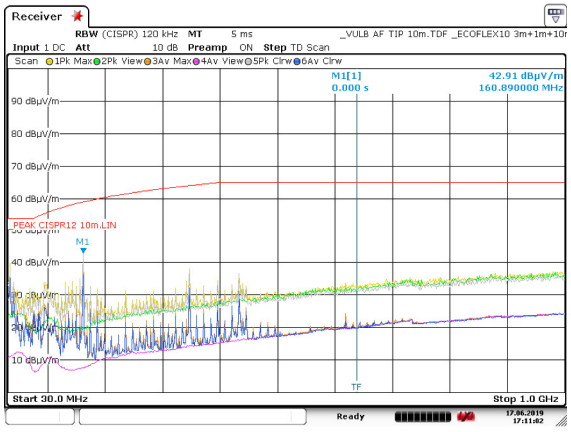

b.

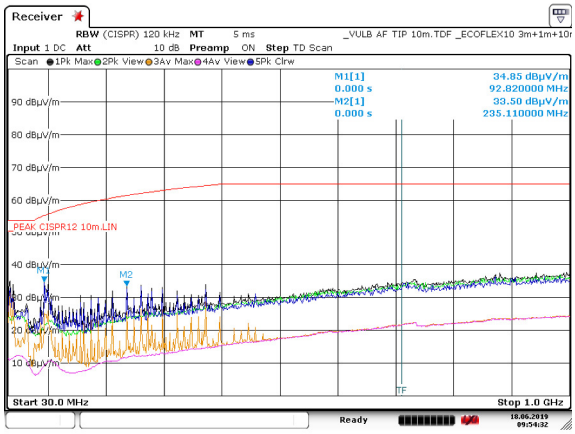

c.

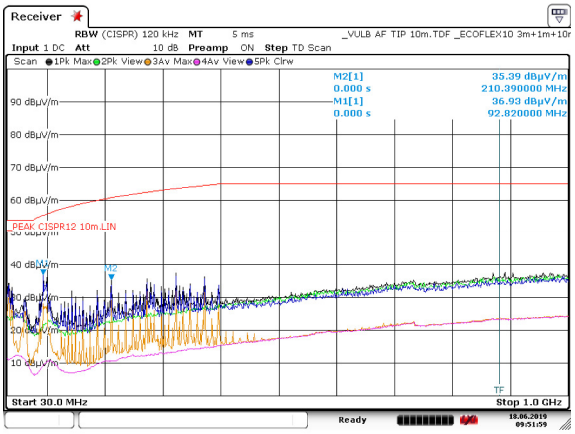

d.

Figure 8: Radiated emissions (30-1000MHz), EV ON, 12V system (safe state, all lights ON), V-pol (a) left and (b) right, H-pol (c) left and (d) right

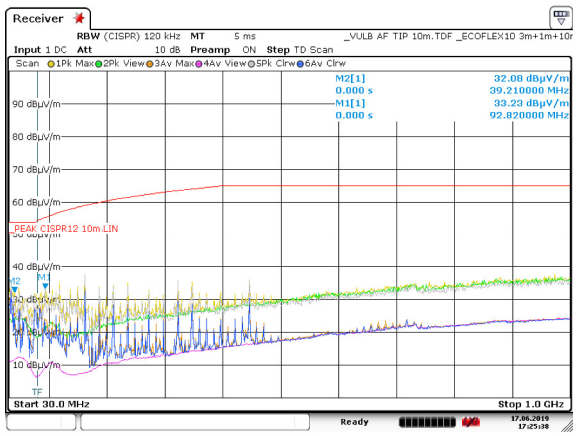

a.

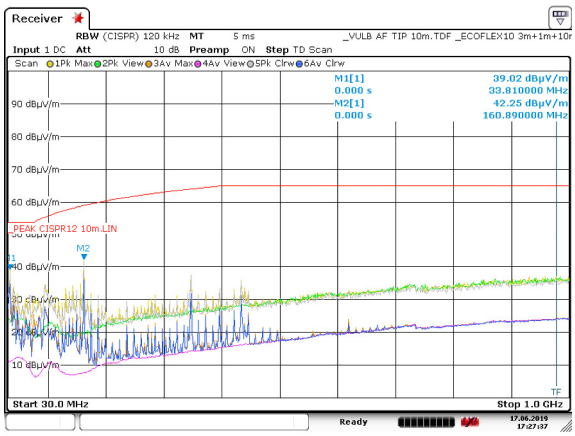

b.

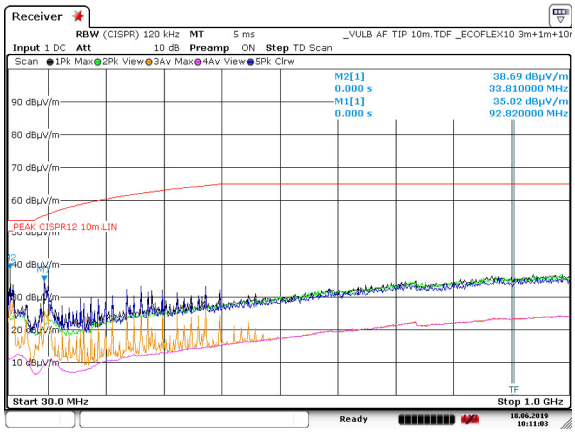

c.

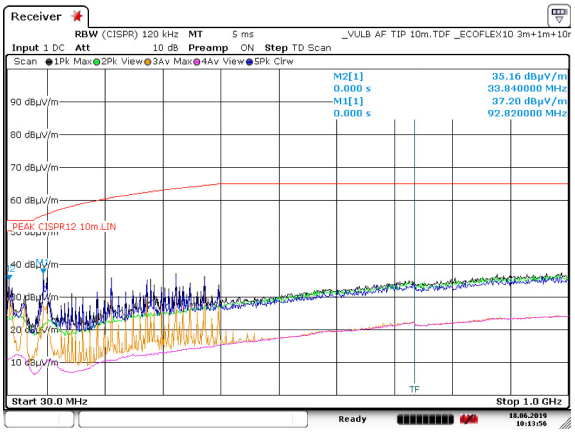

d.

Figure 9: Radiated emissions (30-1000MHz), EV ON, 12V system (safe state, brake, all lights ON), V-pol (a) left and (b) right, H-pol (c) left and (d) right

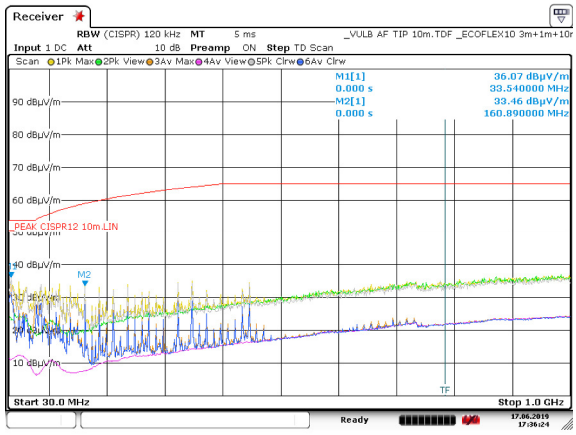

a.

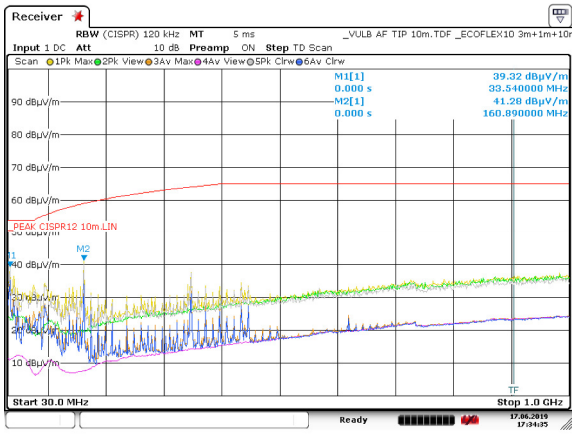

b.

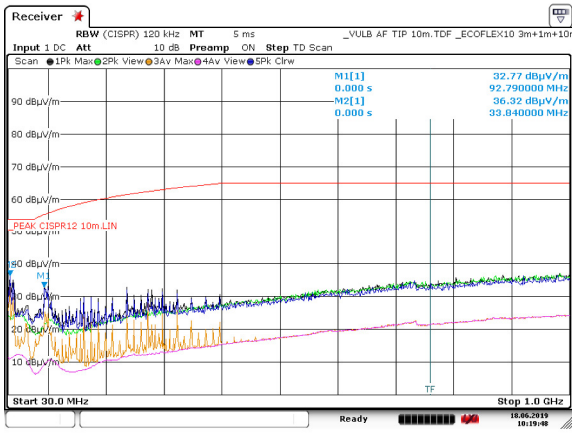

c.

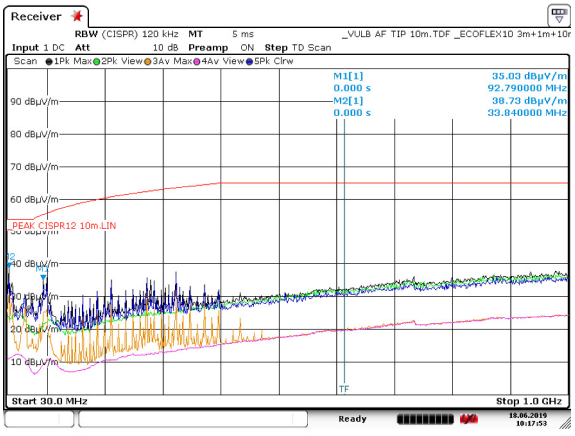

d.

Figure 10: Radiated emissions (30-1000MHz), EV ON, 12V system (motor state, idle), V-pol (a) left and (b) right, H-pol (c) left and (d) right

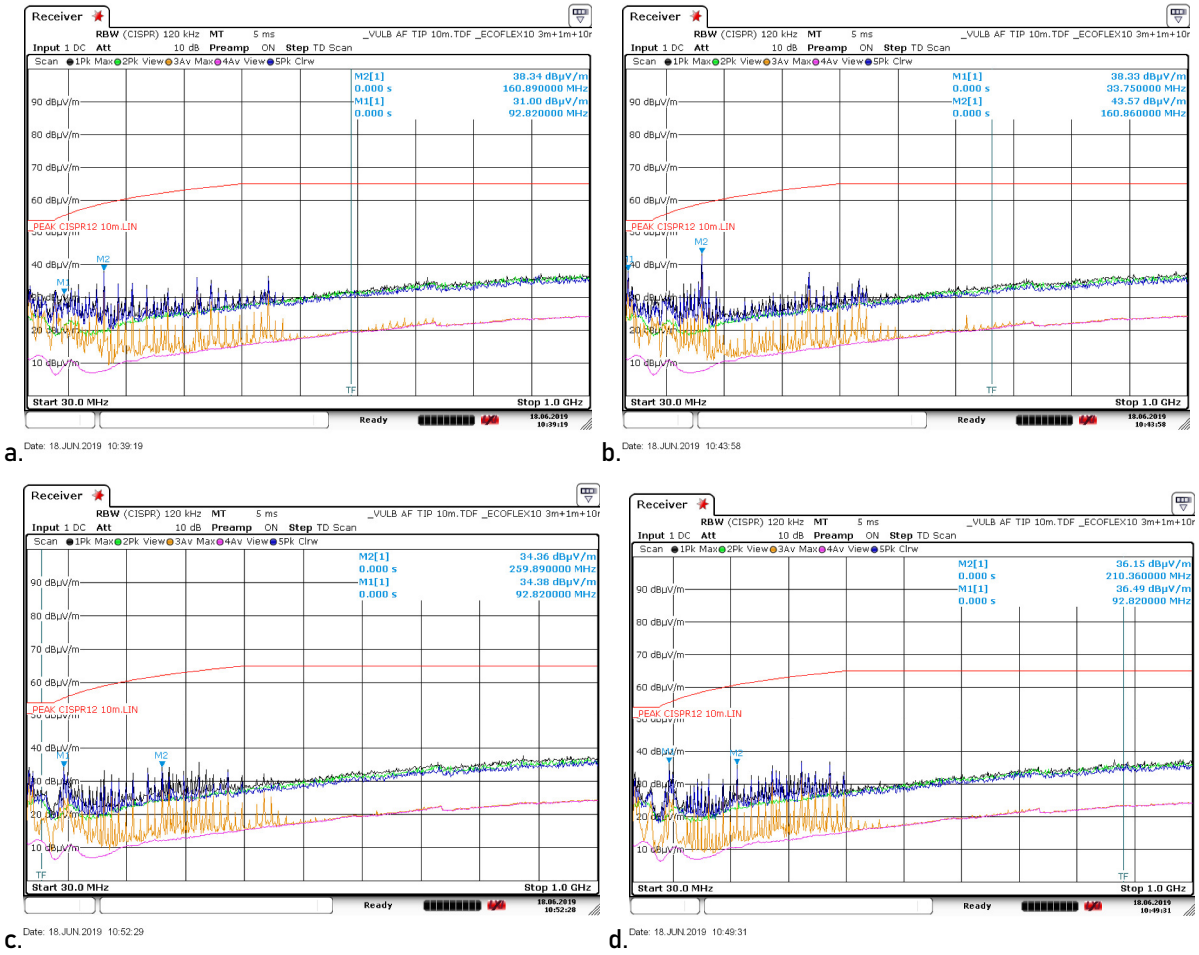

During the different idle conditions, Figures 6 to 10, the vehicle generated primarily narrow band harmonics, which were extended up to around 500MHz. The strongest emissions were observed at 33.81MHz, 92.82MHz and 160.89MHz. The different operating states of the vehicle did not affect drastically or contributed in a different way to the EMI profile of the vehicle.

4.1.2 Driving conditions at constant speeds[2]

Figure 11: Radiated emissions (30-1000MHz), 10km/h (cruise control), V-pol (a) left, (b) right, H-pol (c) left, (d) right

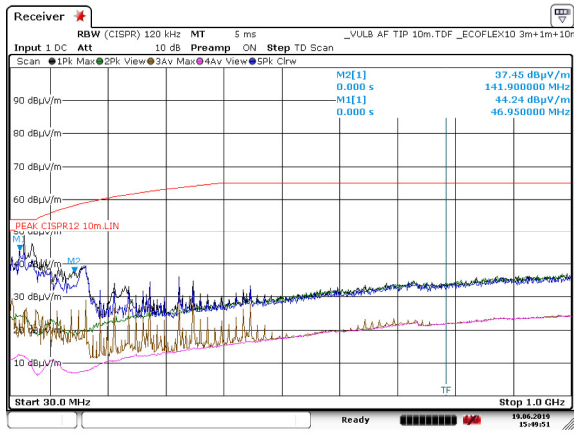

a.

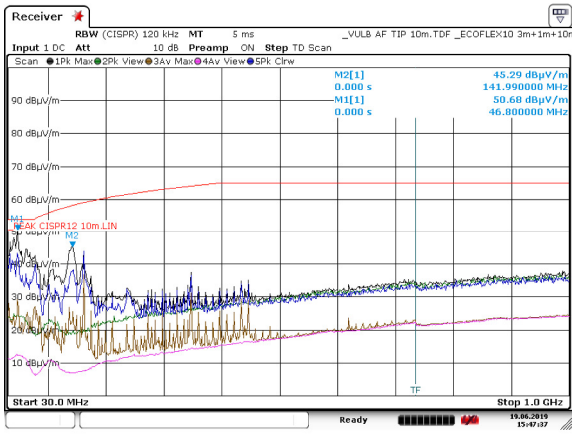

b.

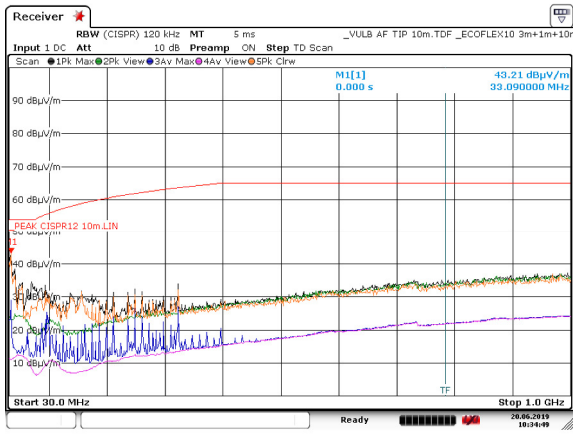

c.

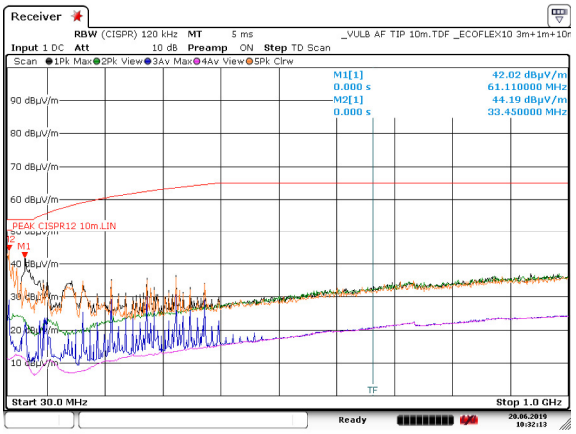

d.

Figure 12: Radiated emissions (30-1000MHz), 20km/h (cruise control), V-pol (a) left, (b) right, H-pol (c) left, (d) right

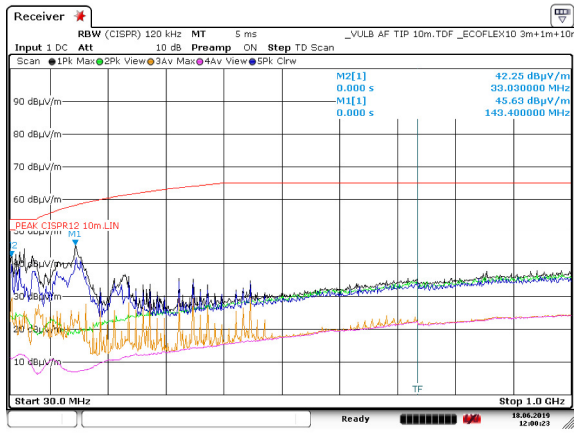

a.

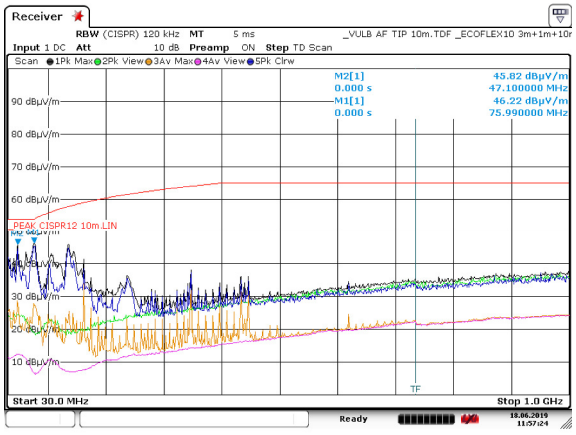

b.

[2] During driving, CISPR 12 requires that the vehicle is tested at a constant speed of 40km/h only. EMC tests at other constant speeds presented on this Section were carried out for the purpose of pre-normative research.

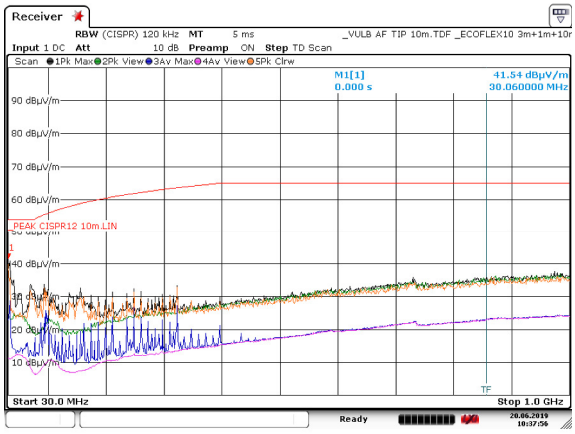

c.

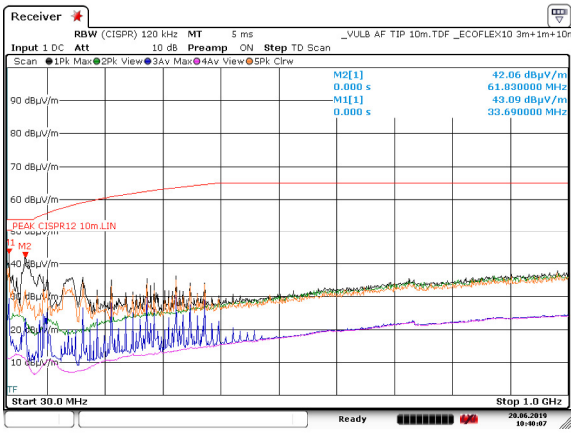

d.

Figure 13: Radiated emissions (30-1000MHz), 30km/h (cruise control) V-pol (a) left, (b) right

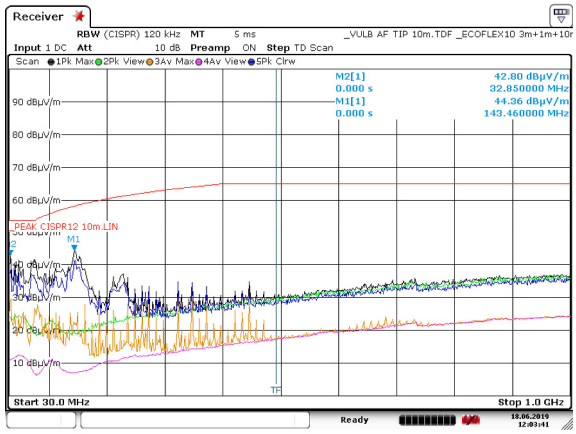

a.

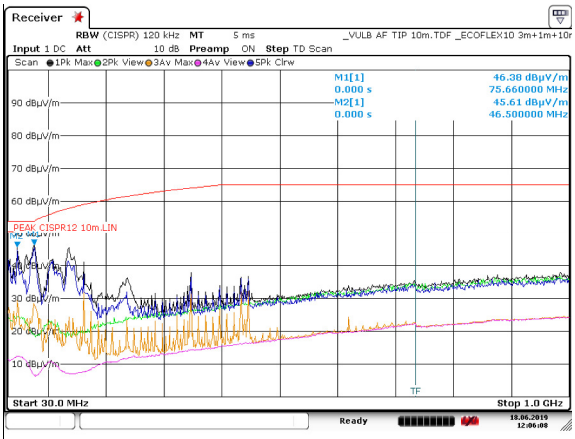

b.

Figure 14: Radiated emissions (30-1000MHz), 40km/h (cruise control)
V-pol (a) left, (b) right, H-pol, (c) left (note: one drive motor OFF), (d) right

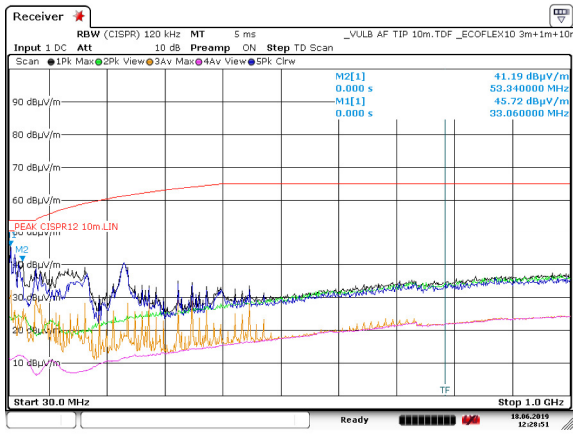

a.

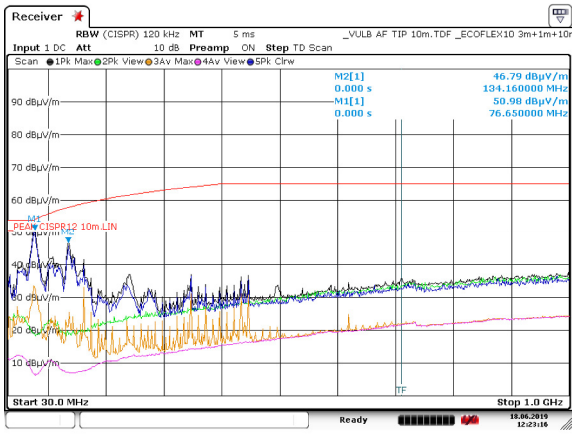

b.

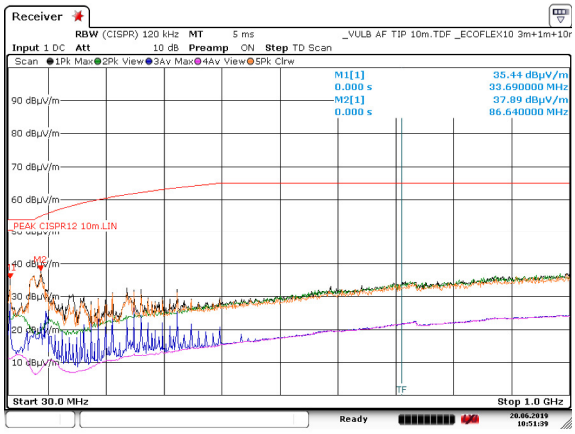

c.

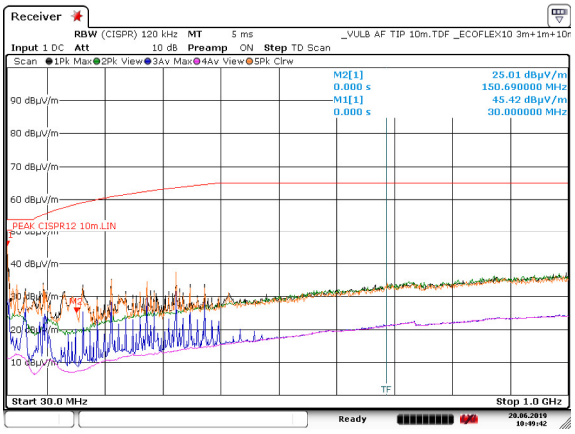

d.

Figure 15: Radiated emissions (30-1000MHz), 60km/h,
V-pol (manual drive) (a) left, (b) right, H-pol (cruise control), (c) left, (d) right (note: one drive motor OFF)

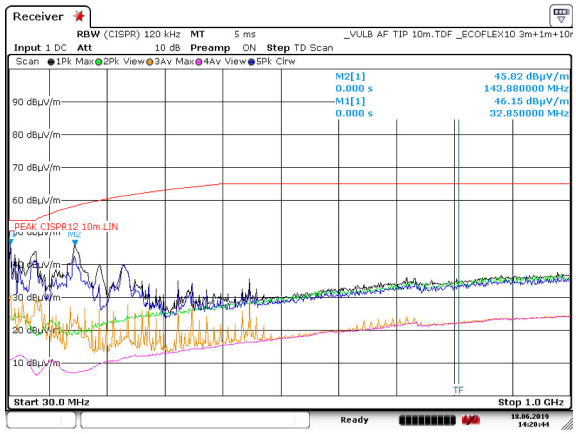

a.

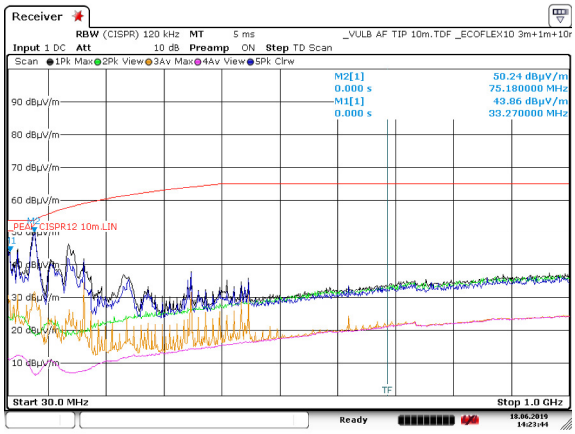

b.

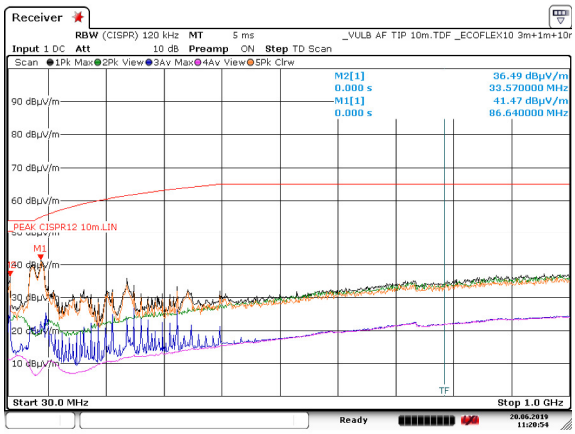

c.

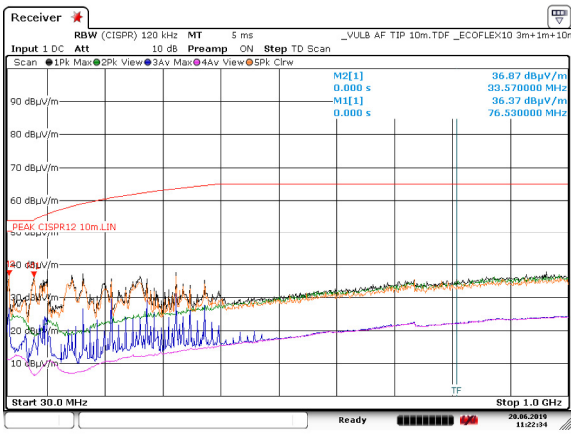

d.

Figure 16: Radiated emissions (30-1000MHz), 80km/h,
V-pol (manual drive) (a) left, (b) right, H-pol (cruise control), (c) left, (d) right

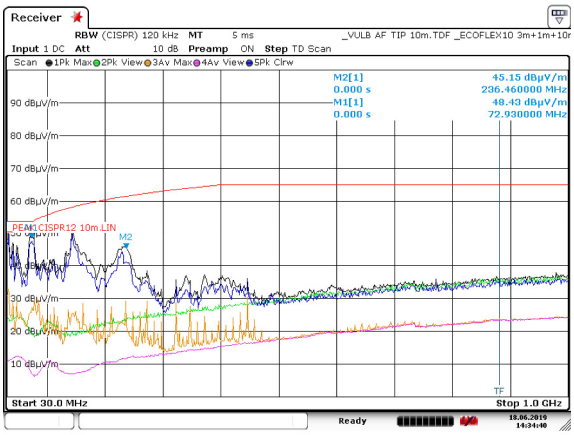

a.

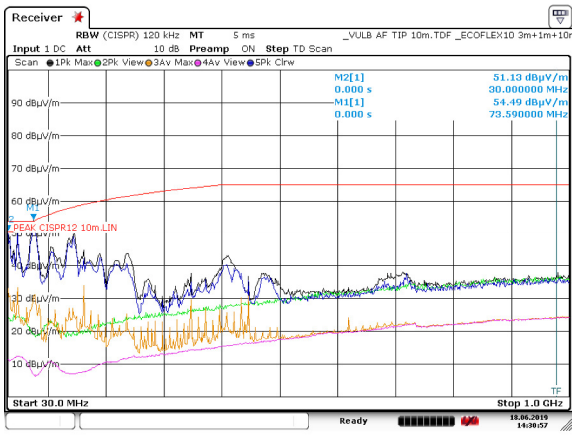

b.

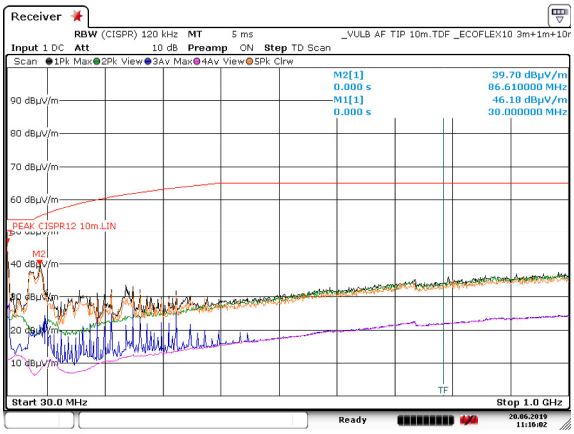

c.

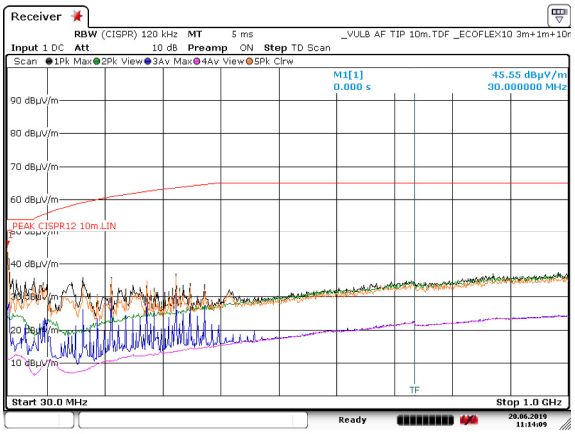

d.

Figure 17: Radiated emissions (30-1000MHz), 80km/h (cruise control) V-pol (a) left, (b) right

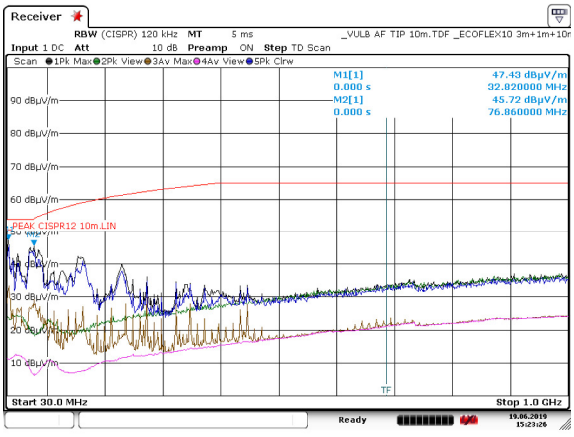

a.

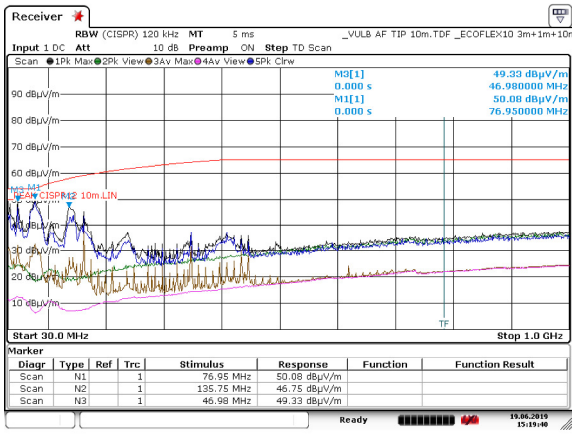

b.

Figure 18: Radiated emissions (30-1000MHz), 100km/h, (cruise control)
V-pol (a) left, (b) right, H-pol (c) left, (d) right

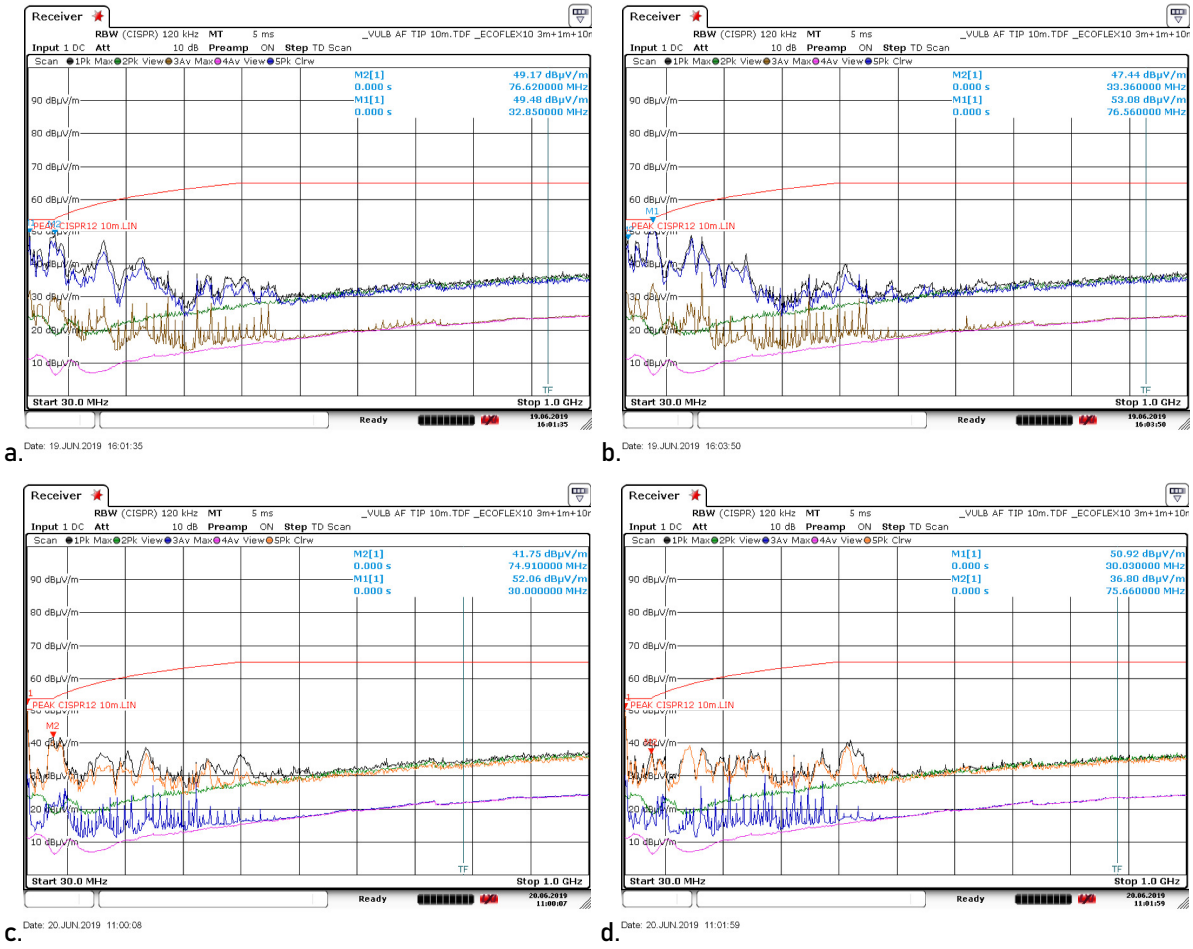

From Figures 11 to 18, it was observed that the EM emissions, mainly broadband, were stronger on the vertical polarization for the frequencies between 30MHz and 200MHz and lower on the horizontal polarization. In addition, comparison of the emissions between idle and speed conditions shows that the level of the EM interference was in general elevated during driving. This could be attributed to the RF interference generated by the DC/AC rectifiers and/or electric traction motors. On the vertical polarization the EM emissions, were mainly originating from the right side of the vehicle. However, at higher speeds i.e. 80, 100km/h both sides of the vehicle were contributing to the EMI as seen from the increased EMI between 30MHz and 200MHz. In some driving conditions, e.g. Figures 16 (a) and (b), 17(b), and 18, the level of the emissions were challenging the CISPR 12 limit around 73-75MHz.

Measurements with two different driving modes at 80km/h, Figures 16 (a) and (b) and Figure 17 (a) and (b) respectively, showed that the vehicle had a relatively more elevated EMI behaviour during *manual* driving compared to *cruise control* mode. This could be attributed to the fact the during cruise control one of the control motor and driving motor, turned off to preserve energy.

4.2 Conducted emissions (150kHz-30MHz) on AC-Line during charging

Evaluation of the conducted RF interference on the AC line using an on-board battery charger was carried out under three different scenarios:

1. 16A AC charging with a DELPHI charger connected in series with the on-board charger
2. 16A AC charging with on-board charger only
3. 32A AC charging with on-board charger only

On Figures 19 to 21, Trace 1 and Trace 2 represented Phase and Neutral lines, respectively, of the AC-line. The red line indicated the corresponding IEC 61851-21-1 limit.

Figure 19: Conducted emissions (150kHz-30MHz), Trace 1=Phase, Trace 2=Neutral, Trace 6=noise floor, ONBOARD charger in series with DELPHI portable charger, (a) QP, (b) Avg. detectors

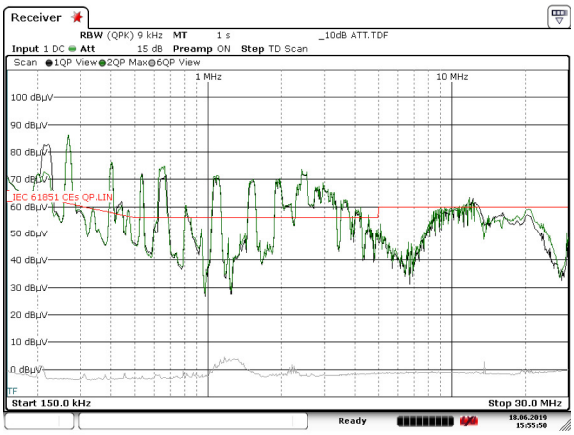

a.

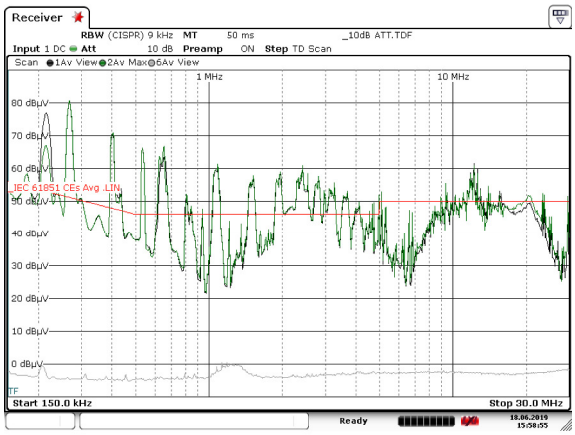

b.

Figure 20: Conducted emissions (150kHz-30MHz), Trace 1=Phase, Trace 2=Neutral, Trace 6=noise floor, ONBOARD charger at I=16A, (a) QP, (b) Avg. detectors

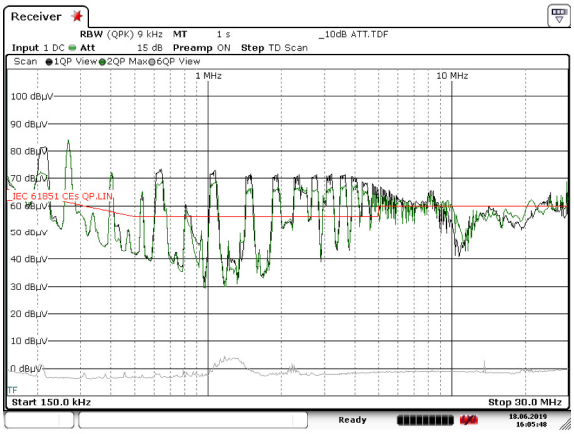

a.

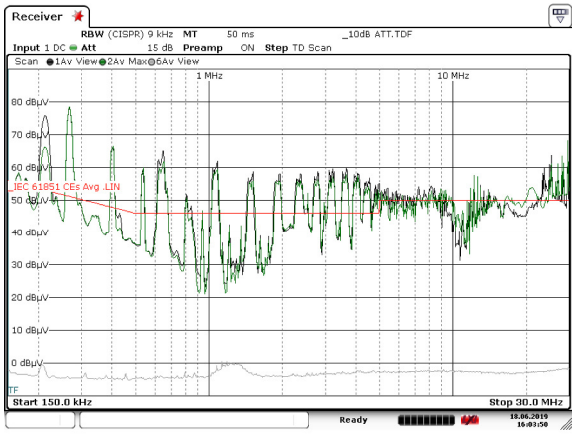

b.

Figure 21: Conducted emissions (150kHz-30MHz), Trace 1=Phase, Trace 2=Neutral, Trace 6=noise floor, ONBOARD charger at I=32A, (a) QP, (b) Avg. detectors

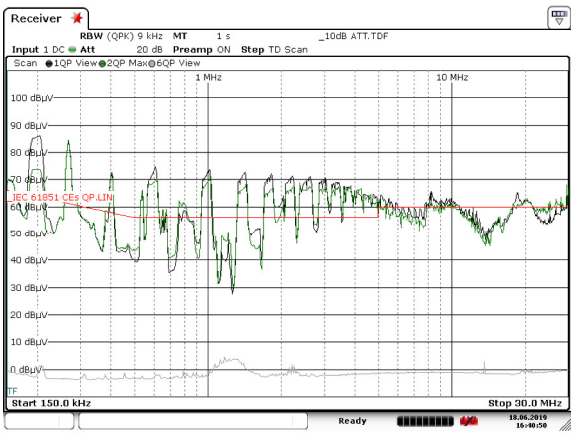

a.

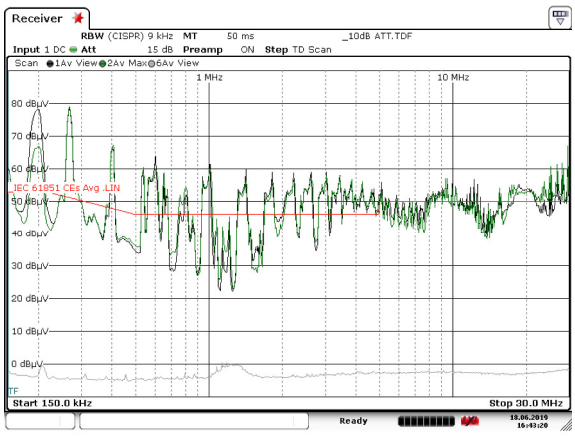

b.

The conducted EM emissions were particularly strong and exceeded the limit both for the quasi-peak and average detector during all charging scenarios. Charging the DC battery with a current of 16A or 32A did not show any noticeable differences on the level of the EM disturbances.

4.3 Exploratory EMC measurements

As stated, additional measurements outside the requirements of the EMC standards were carried out for the purpose of pre-normative and exploratory work described on (Pliakostathis-1 *et al*, 2019) and (Pliakostathis-2 *et al*, 2019). These results can assist and accelerate the EMC troubleshooting process and help to identify the cause of potential EMI issues.

4.3.1 Radiated Emissions (30-1000MHz)

On this part, the max-hold level of the radiated emissions was captured in the frequency domain by performing a full rotation of the vehicle on the turntable during idle and driving conditions, whilst performing a frequency sweep on the EMI receiver from 30MHz to 1GHz.

For each setup, the operating and driving state of the vehicle is described on the title for each Figure below.

4.3.1.1 Idle State

Figure 22: Maximum radiated emissions (30-1000MHz) around the vehicle, EV ON, 12V system (safe state), (a) V-pol, (b) H-pol

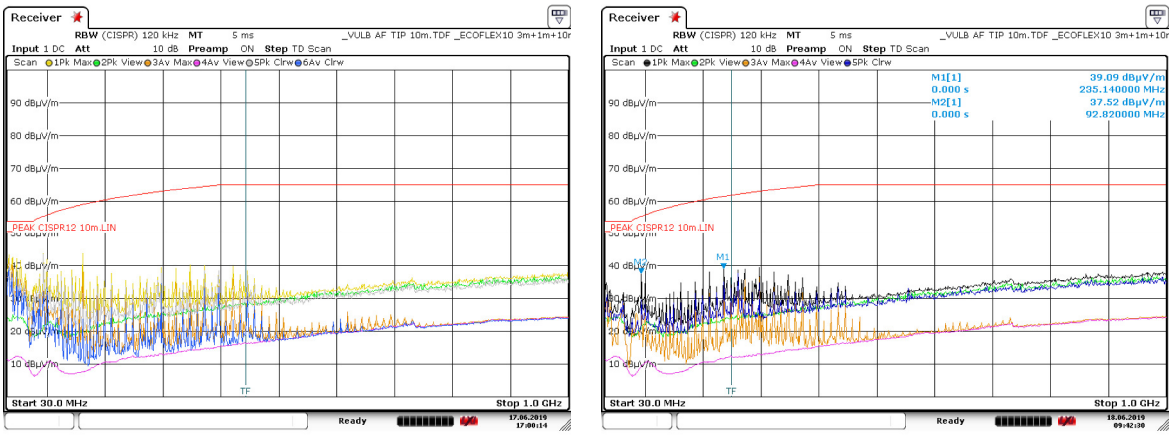

a. b.

Figure 23: Maximum radiated emissions (30-1000MHz) around the vehicle, EV ON, 12V system (safe state, parking light), (a) V-pol (b) H-pol

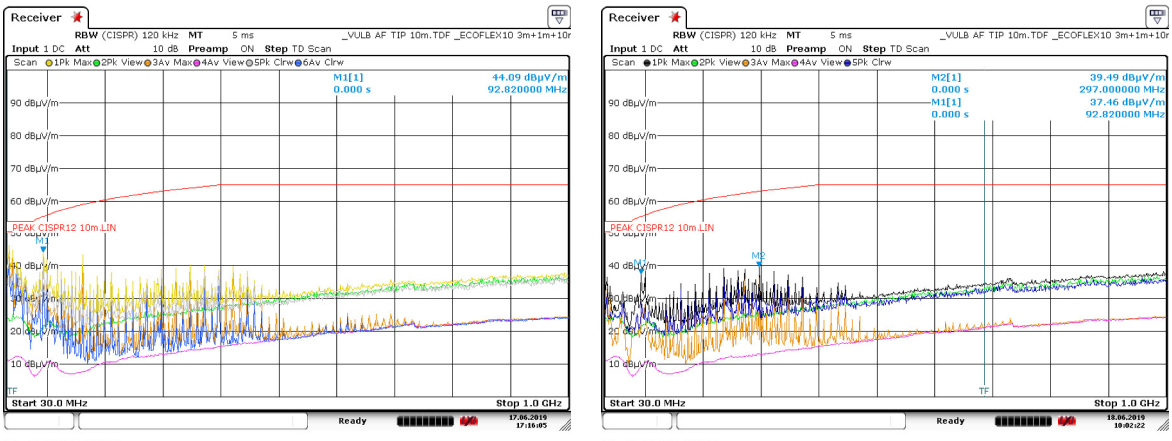

a. b.

Figure 24: Maximum radiated emissions (30-1000MHz) around the vehicle, EV ON, 12V system (safe state, all lights ON), (a) V-pol (b) H-pol

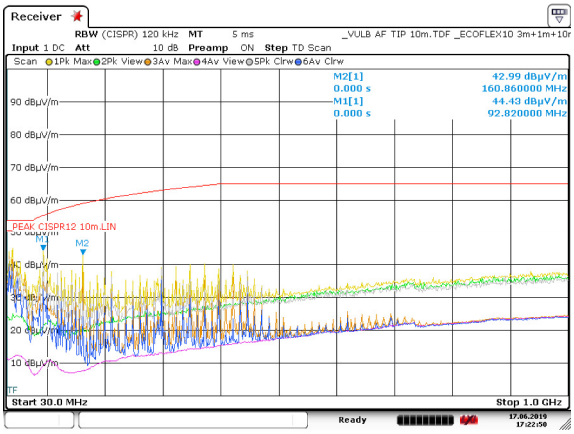

a.

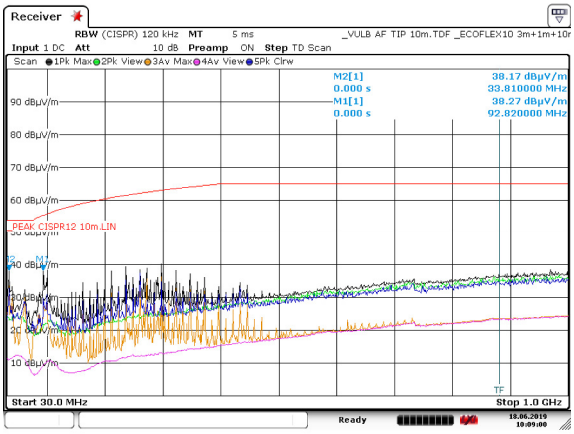

b.

Figure 25: Maximum radiated emissions (30-1000MHz) around the vehicle, EV ON, 12V system (safe state, brake, all lights ON), (a) V-pol (b) H-pol

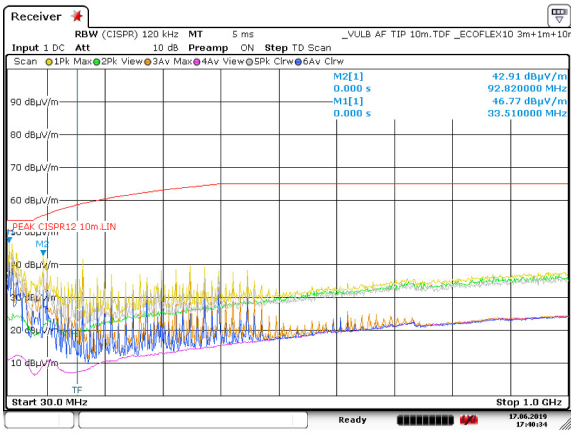

a.

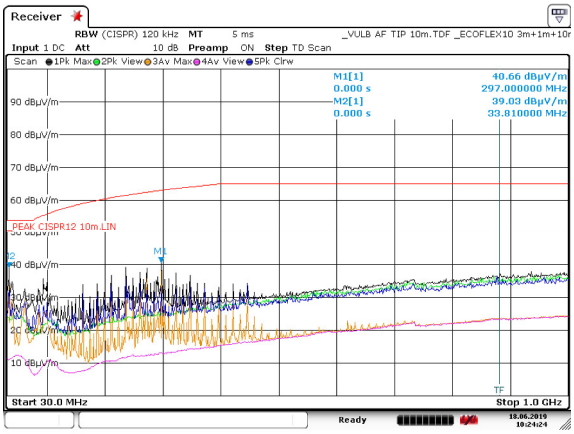

b.

Figure 26: Maximum radiated emissions (30-1000MHz) around the vehicle, EV ON, 12V system (motor state, idle), (a) V-pol (b) H-pol

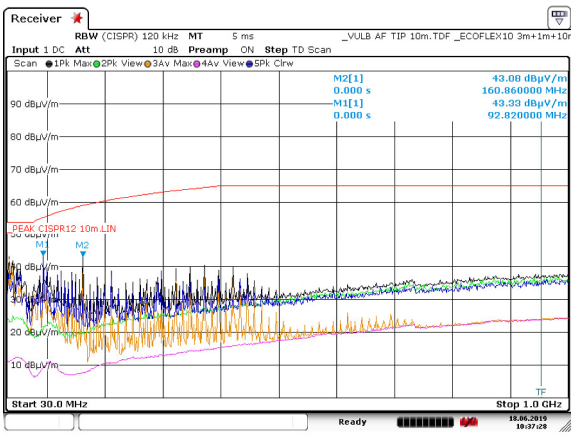

a.

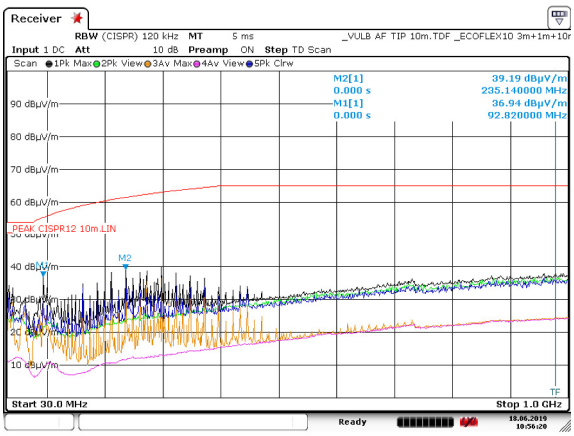

b.

4.3.1.2 Drive State

Figure 27: Maximum radiated emissions (30-1000MHz) around the vehicle at 10km/h (a) V-pol, (b) H-pol

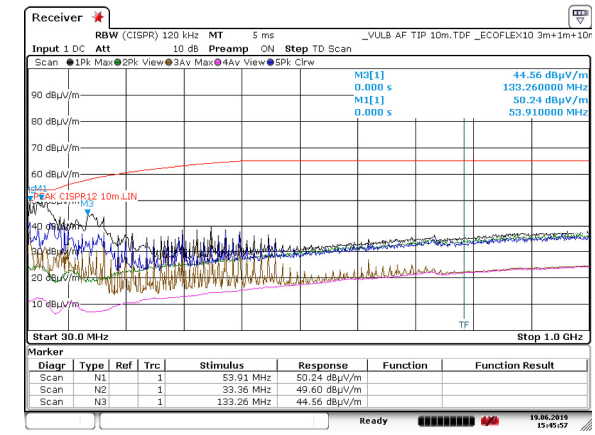

a.

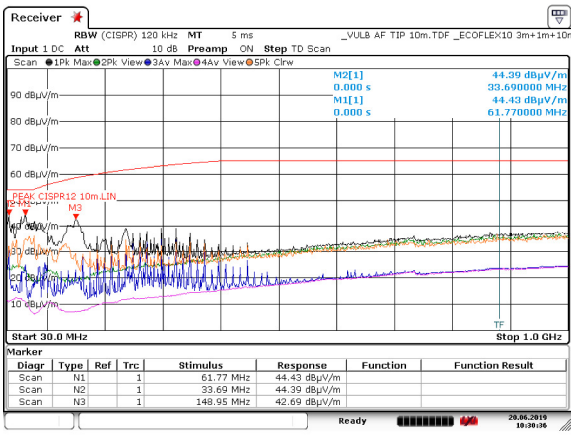

b.

Figure 28: Maximum radiated emissions (30-1000MHz) around the vehicle at 20km/h (a) V-pol, (b) H-pol

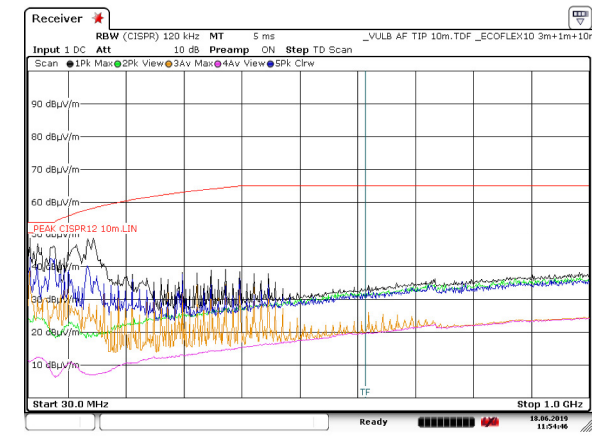

a.

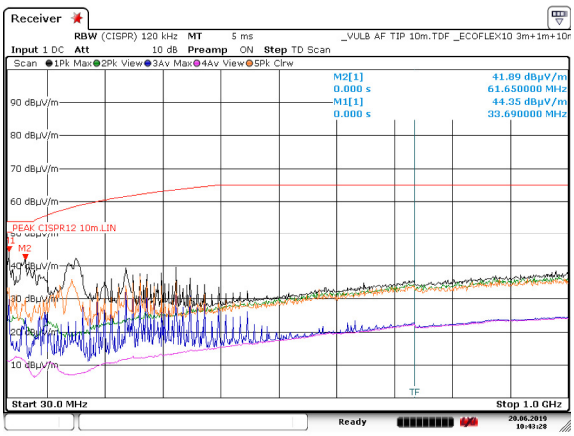

b.

Figure 29: Maximum radiated emissions (30-1000MHz) around the vehicle at 40km/h (a) V-pol, (b) H-pol

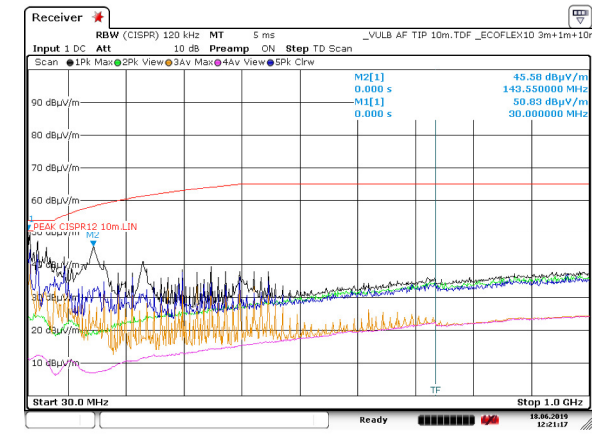

a.

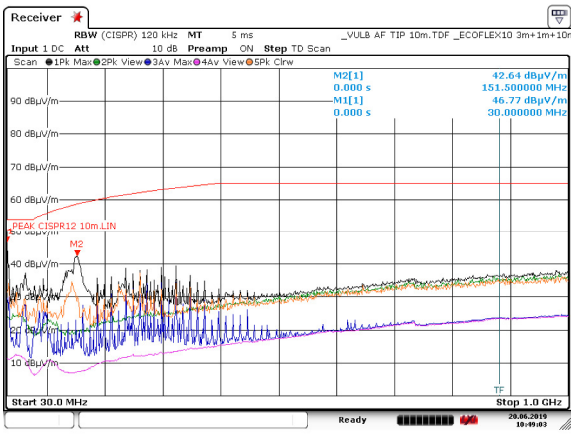

b.

Figure 30: Maximum radiated emissions (30-1000MHz) around the vehicle at 60km/h (a) V-pol, (b) H-pol

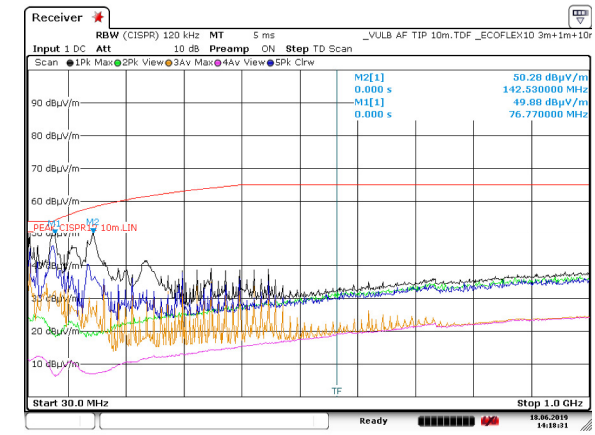

a.

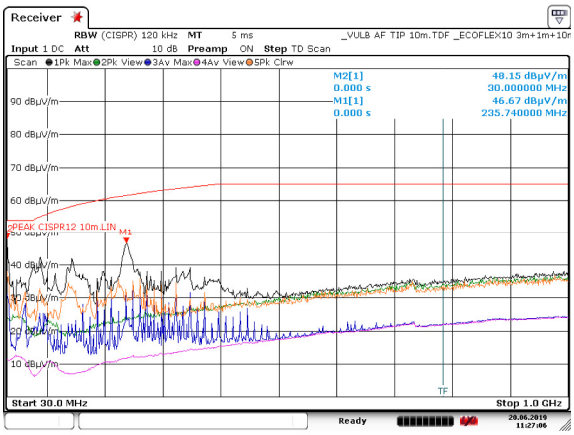

b.

Figure 31: Maximum radiated emissions (30-1000MHz) around the vehicle at 80km/h (a) V-pol, (b) H-pol

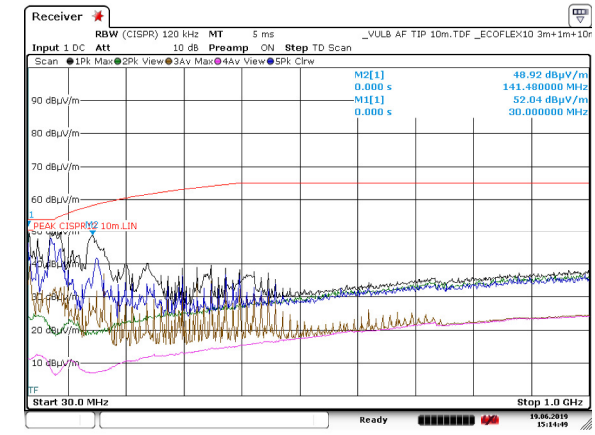

a.

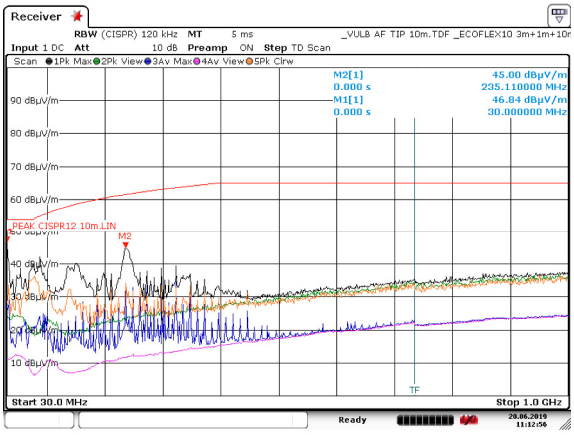

b.

Figure 32: Maximum radiated emissions (30-1000MHz) around the vehicle at 100km/h (a) V-pol, (b) H-pol

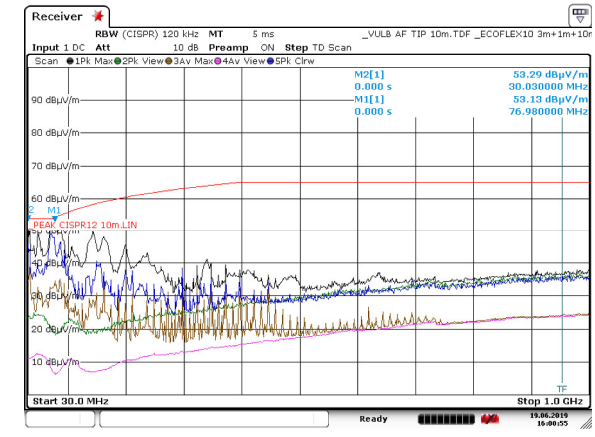

a.

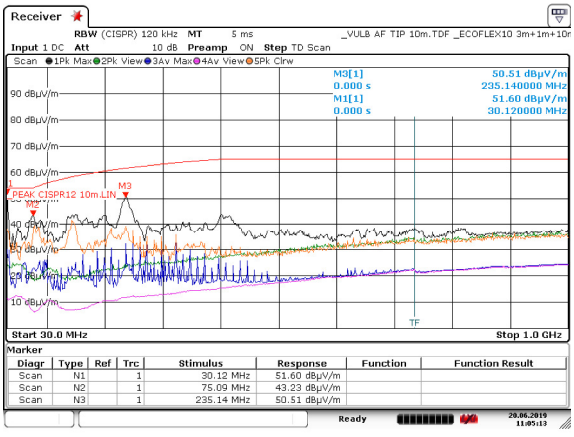

b.

During idle conditions, the emissions were dominated by narrowband interference, which was concentrated up to around 500MHz, while in the driving state both narrowband and broadband interference was noticed. On the latter condition, this broadband interference was elevated with the velocity of the vehicle. For example, between 10km/h and 60km/h the emissions were generally limited up to 500MHz, while at 80km/h and 100km/h the emissions were extended up to around 800MHz. The strongest peaks were observed close to 32MHz, 76.98MHz, 92.82MHz, 141.48MHz, 151.5MHz, 160.86MHz and 235MHz,

4.3.2 Radiated Emissions (150kHz – 30MHz) during constant speed

On this setup, the maximum radiated emissions between 150kHz and 30MHz were monitored with the active monopole E-field antenna when the vehicle was rotated by the turntable and driven with a constant speed of 40km/h.

Figure 33: Maximum radiated emissions (150kHz – 30MHz) around the vehicle at 40km/h (manual driving)

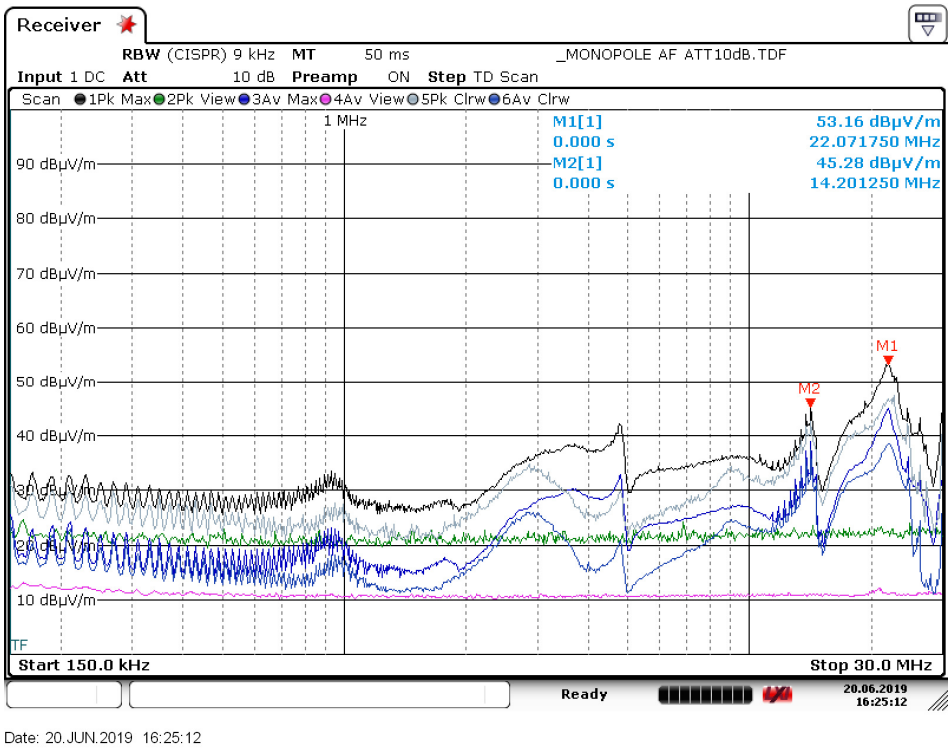

The results of the radiated emissions below 30MHz identified emissions which were spanning from around 2MHz up to 28MHz. The strongest emissions were at 4.8MHz, 14.2MHz and 22.07MHz. Due to the limited time availability of the vehicle, no additional radiated emissions tests were carried out below 30MHz.

4.3.3 Time-domain analysis of radiated emissions during dynamic driving conditions

The time-dependency between the radiated emissions and the vehicle's driving state, according to the method proposed in (Pliakostathis-1 *et al*, 2019), presented on this Section, provides a direct and immediate information about the EM contribution of each driving phase i.e. motor switch-ON, driving/reverse setting, acceleration, constant speed, deceleration and switching OFF. Such results of these measurements were extracted by merging the electric field levels monitored by the EMI receiver with the data generated by the chassis dynamometer, which included vehicle speed, power on the wheels and acceleration (or deceleration).

Three different driving scenarios were evaluated:

1. Short driving cycle up to 80km/h
2. Multiple constant speeds up to vehicle's top speed (right side) and
3. Multiple constant speeds up to vehicle's top speed (left side)

Figure 34: Electric field (radiated emissions) variation in time with vehicle's driving state up to 80km/h (aggressive acceleration), right side, V-pol

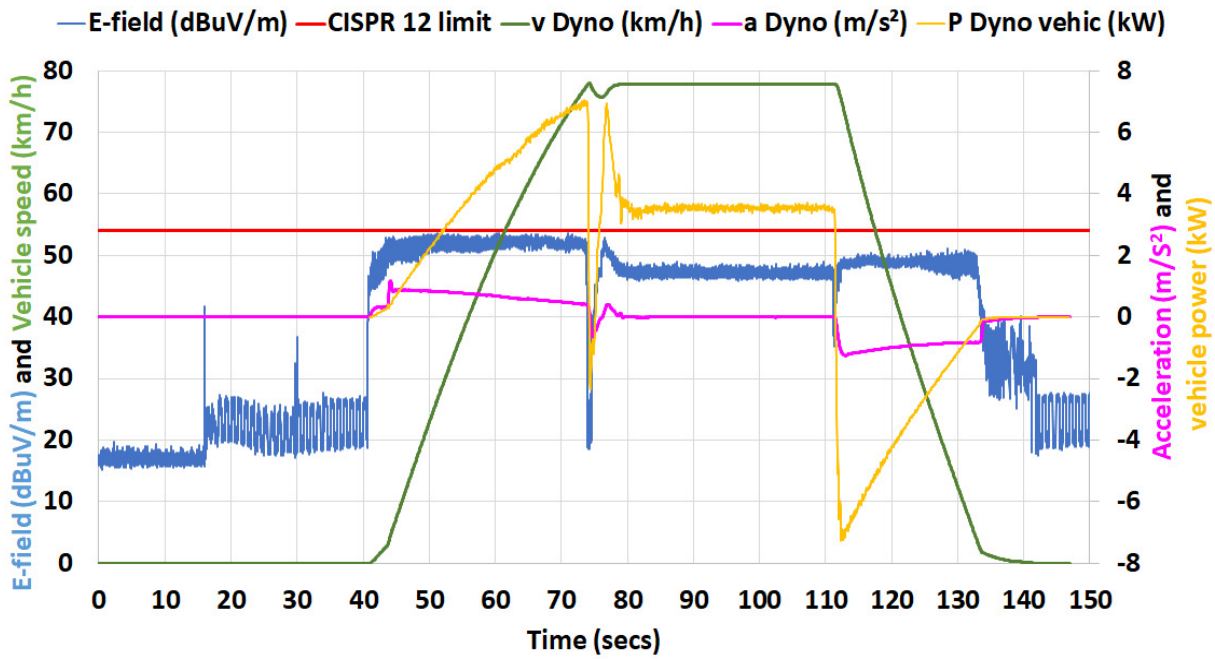

Figure 35: Electric field variation in time with vehicle's driving state up to vehicle's maximum speed (≈90km/h), right side, V-pol

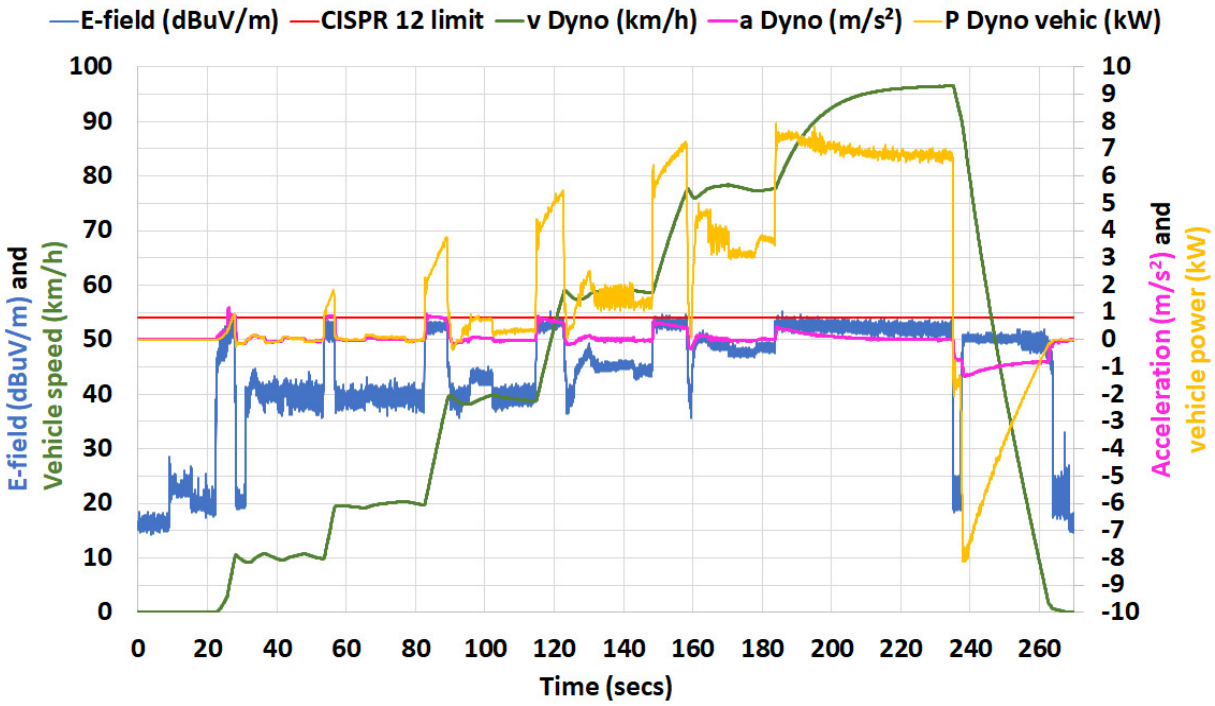

Figure 36: Electric field variation in time with vehicle's driving state up to vehicle's maximum speed (≈90km/h), left side, V-pol

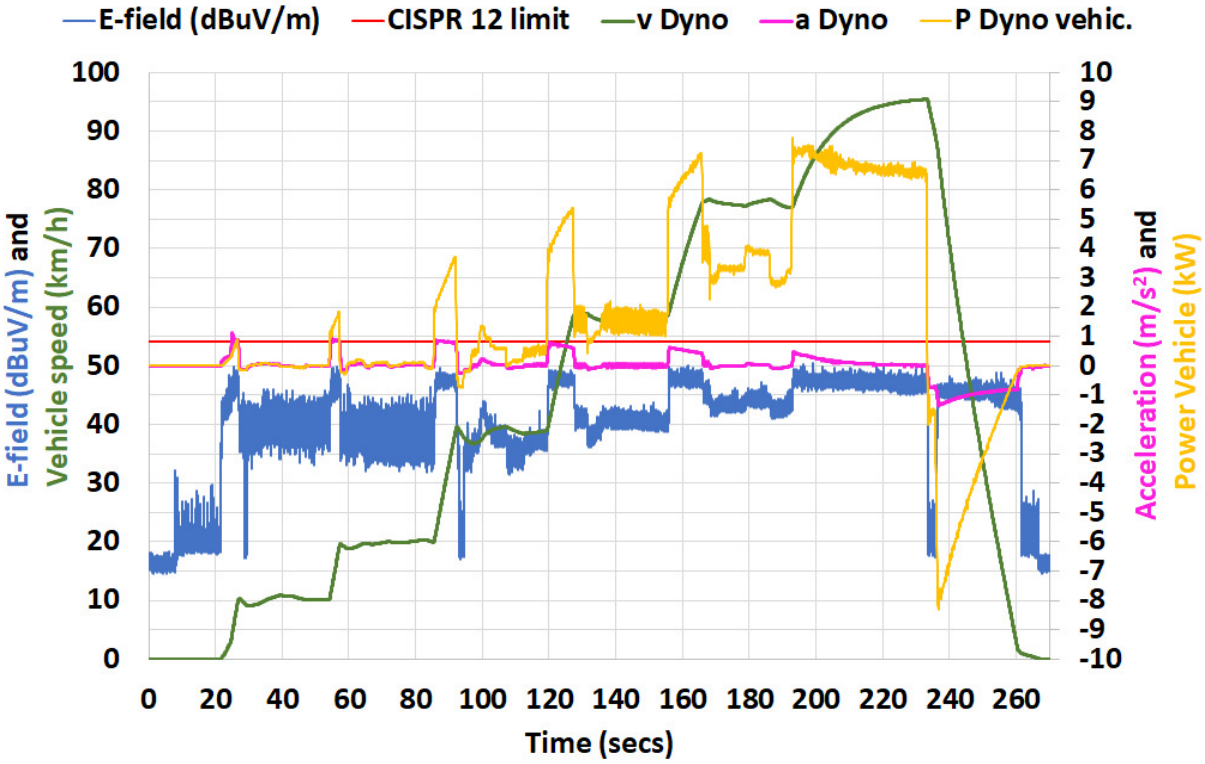

Investigation of the individual traces on Figures 34, 35 and 36, indicate that there was a very strong correlation between the E-field and the vehicle's acceleration. On the other hand higher constant speeds did not result in the same proportion an increase of the E-field. This could be justified from the following situation: The power and battery management system of the vehicle utilize fast switching pulses for the conversion of the DC voltage into AC voltage. These pulses contain multiple high-frequency harmonics, which propagate in the form of common or differential type RF noise across the wires with the potential to radiate on the environment (wire-antenna effect at EM frequencies). This EM radiation has a strength proportional to the amount of the *RF currents* that flow through these the interconnected wires of the power management system. As *acceleration* is very much depended on the magnitude of the battery current and hence on the content of the high RF frequency harmonic currents, it justifies that strong velocity changes i.e. acceleration/deceleration, produced higher electric fields.

The highest level of the emissions was stronger on the right (Figure 35) and less on the left (Figure 36) side of the vehicle, i.e. 55dBuV/m and 50dBmV/m, respectively, observed during the acceleration phase. The irregular pattern of the EM emissions at 40km/h and 60km/h, Figures 35 and 36, was attributed to the driver's non-uniform pressing force on the accelerator.

Furthermore it was observed that the EM emissions were lower during constant speed, than during the acceleration and deceleration phases. This is indicated by the 'squared' window sections of the E-field during the acceleration phase, for example at 22secs, 55secs, 82secs, 115secs and 149 secs on Figure 35. In addition, the emissions during constant speed tended to increase with the speed from 10km/h to 95km/h, this is particularly evident on the right side of the vehicle, Figure 35, when the emissions were around 42dBuV/m at 10km/h, 20km/h and 40km/h and then were elevated to 45dBuV/m and 50dBuV/m, at 60km/h and 80km/h respectively. This observation comes in agreement with the set of measurements presented on Sections 4.1.2 and 4.3.2.1, which also showed that the emissions tended to be proportional to vehicle's velocity.

The short bursts of the E-field at the start of the measurement were generated by the switch-ON action of the vehicle, e.g. Figure 34 at 15secs. Between the switch-ON instance and prior to the start of the acceleration the E-field variations were caused by the gear change action for preparation to driving, e.g. Figure 34 at 30 secs.

4.3.4 Radiation pattern (azimuth scan) around the vehicle during driving/charging

Plots of the radiated emissions around the vehicle (Pliakostathis-1 *et al*, 2019) can point to the areas around the chassis of the vehicle that contribute to the far-field emissions. The first and second part of this Section discusses the radiated emission results during charging and driving conditions, respectively. The plots were extracted by combining the electric field level data of the EMI receiver with the value of the angle of the turntable during a complete 360 degrees rotation at constant angular speed.

4.3.4.1 Charging

During AC charging (32A) firstly the radiated emissions levels at four observation angles around the vehicle (front, left, rear, right) were measured up to 1GHz for the vertical and horizontal polarization, as shown on Figure 37. The applicable limit line, shown in red colour on the Figures, is defined in accordance with IEC 61851-21-1 standard.

Figure 37: Electric field emissions from the vehicle during charging (32A)
(a) V-pol, (b) H-pol [Traces: 1.Front, 2.Left, 3.Rear, 4.Right]

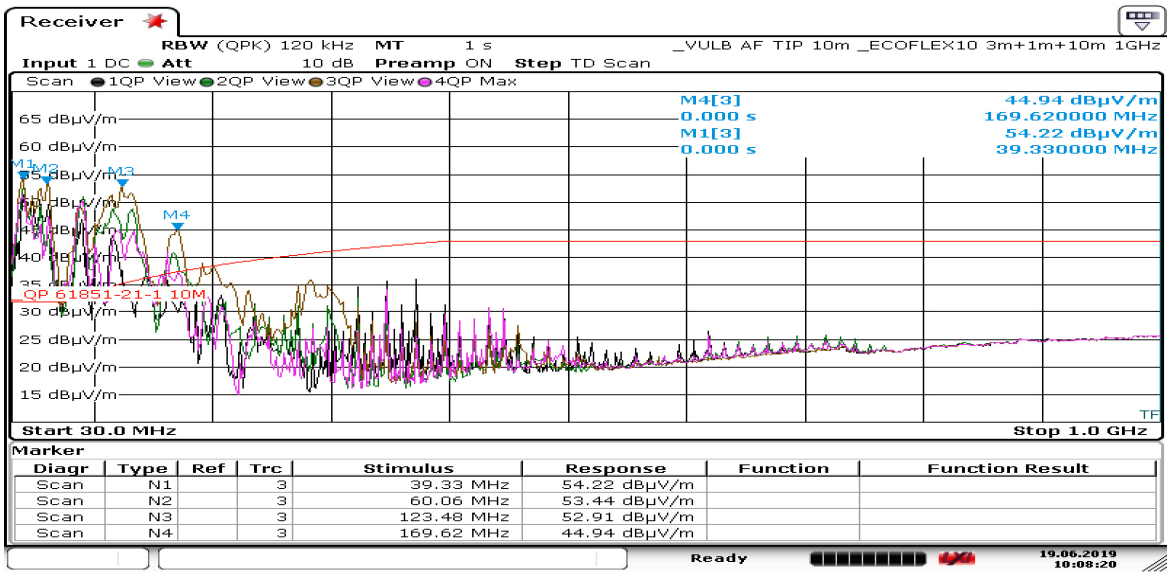

Date: 19.JUN.2019 10:08:21

(a)

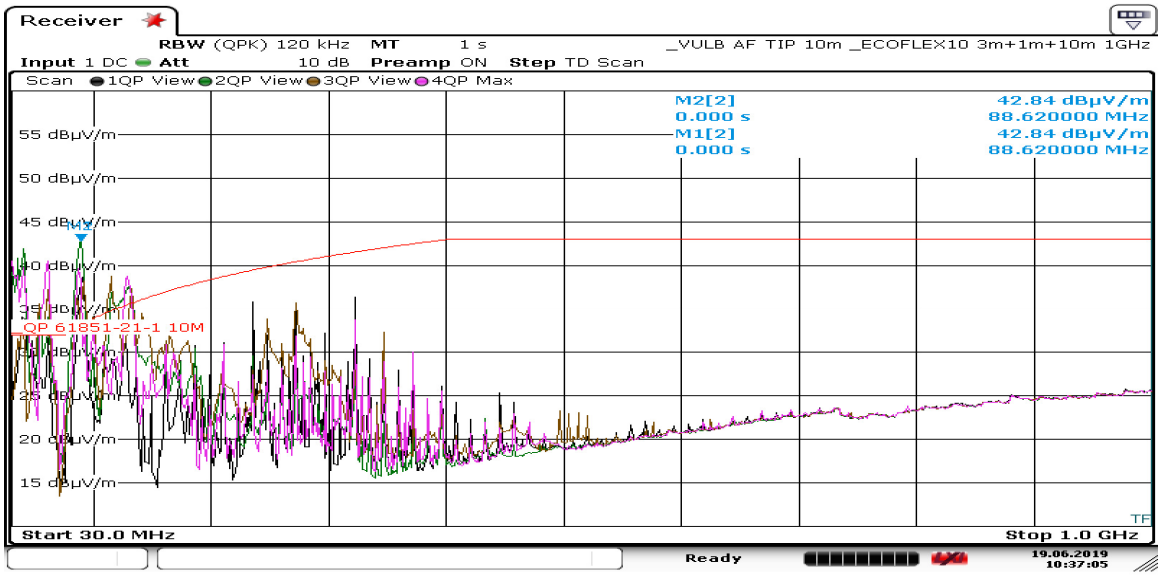

Date: 19.JUN.2019 10:37:05

(b)

Observing each of the 4 traces on Figure 37(a), it is seen that in the *vertical* polarization the rear side of the vehicle dominates at 39.33MHz, 60.06MHz 123.48MHz and 169.62MHz with worse case peaks reaching about 55dBuV/m, or about 10dB above the corresponding IEC 61851-21-1 limit. In the *horizontal* polarization, Figure 37(b), the emissions were stronger on the left side of the setup with maximum field level of 42.84dBuV/m at 88.62MHz. For all test conditions, the emissions exceeded the limit due to strong interferences concentrated below 200MHz.

Results of the radiation patterns, based on the test methodology described on (Pliakostathis-2 *et al*, 2019), at 39.33MHz and 123.48MHz in the vertical polarization and 88.62MHz in the horizontal polarization during charging, are shown on Figure 38.

Figure 38: E-field (dBuV/m, QP detector) azimuth plot around the vehicle during charging (32A) at different frequencies [the equation used to calculate the IEC 61851-21-1 limit for each frequency with the QP detector was defined on Section 2]

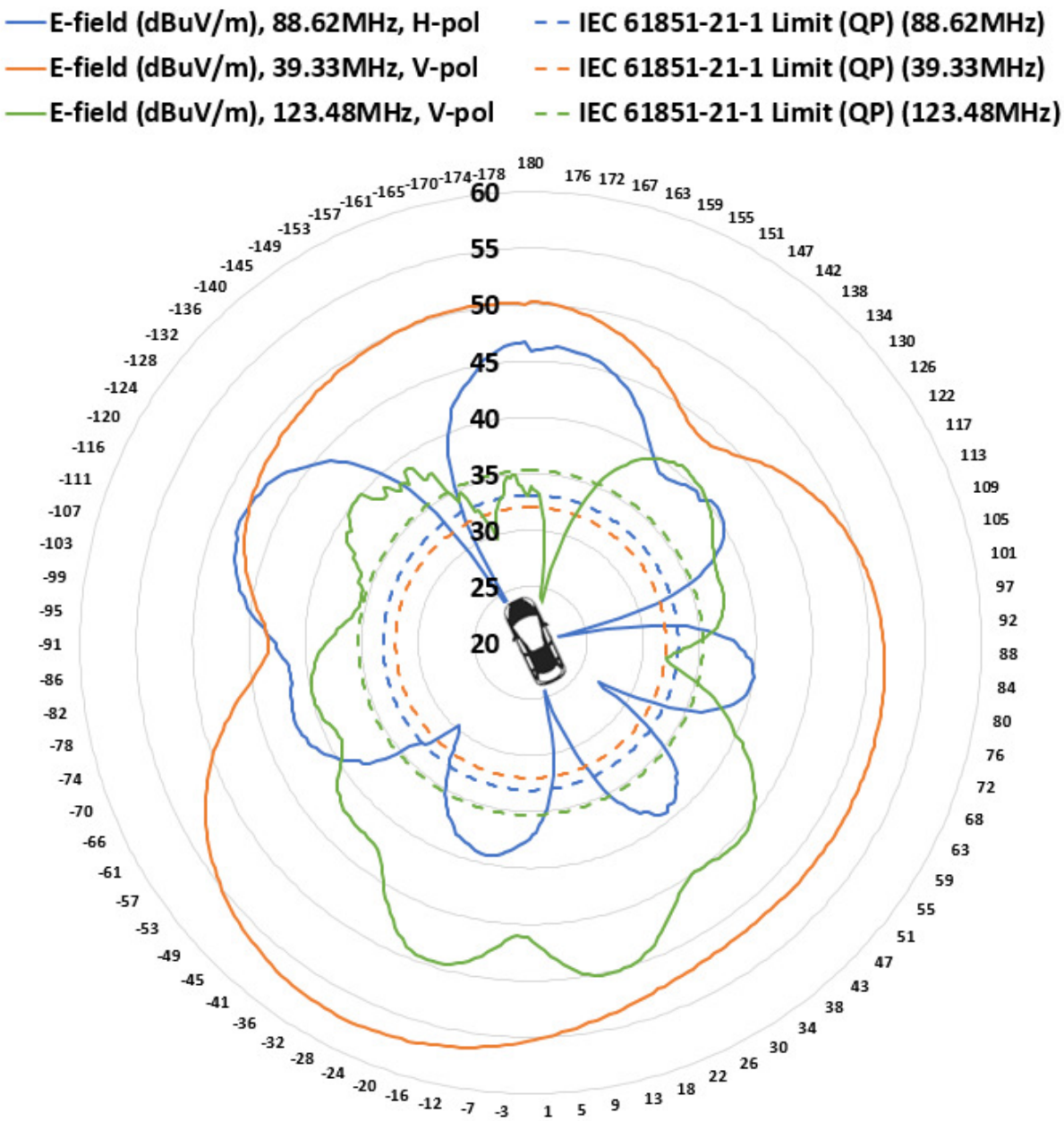

It is seen that in the vertical polarization, the electric field was stronger around the vehicle on the rear-left side with field strength exceeding 57dBuV/m, or about 5dB above the rear side of the vehicle and 23dB above the IEC 61851-21-1 limit. Note that our radiation pattern test method has managed to identify the actual worst case emission angles, which would have missed with only a 4-side scan, For example, at 39.33MHz, Figure 37(a), the peak electric field strength was 54.22dBuV/m from the rear, while the far field scan revealed that the actual peak emission at this frequency was close to 57dBuV/m from the rear-left side. In a similar analogy, at 88.62MHz, Figure 37(b), the peak electric field was 42.84dBuV/m from the left side of the setup, while the 360 degrees azimuth scan, Figure 38, indicated that the actual peak at this frequency was ≈48dBuV/m, originating from the front-left and front-right side of the setup.

4.3.4.2 Driving

The radiation pattern plots during constant speed driving were extracted for three different vehicle speeds i.e. at 40, 80 and 100km/h. These are shown on the traces on Figure 39.

Figure 39: E-field (dBuV/m, peak detector) azimuth plot around the vehicle at different constant speeds and frequencies [the equation used to calculate CISPR 12 limit for each frequency with the Peak detector was defined on Section 2]

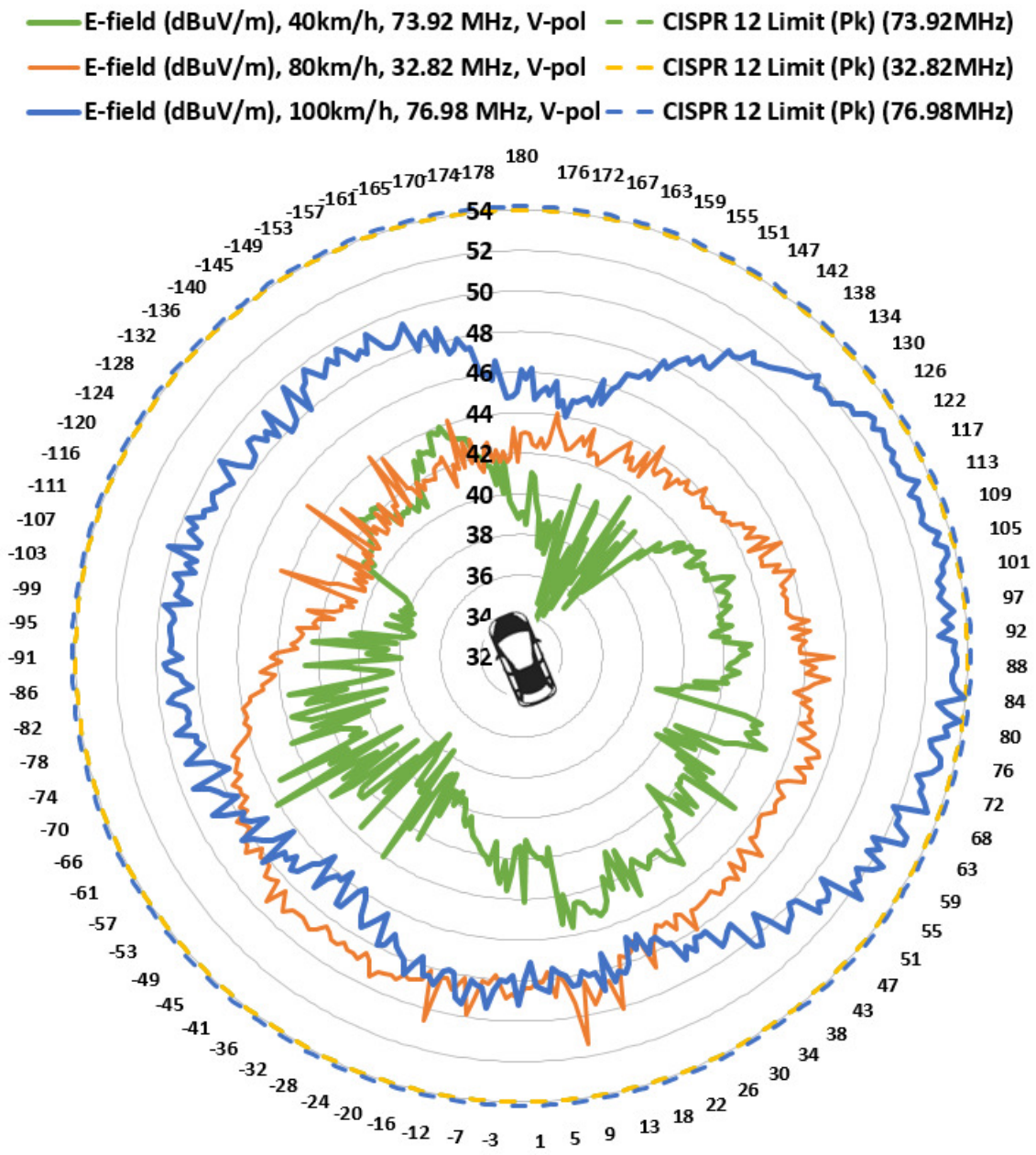

At the highest speed of 100km/h, the EMI levels were strongest at the right and rear-right side of the vehicle. Notice that measurements solely on the left and right side of the vehicle, does not provide a guarantee that the worst-case emissions can be captured, hence confirming the usefulness of the vehicle's radiation pattern measurement. For example, at 80km/h, the strongest emissions tended to originate from the rear and rear-side of the vehicle, with peaks from the rear side which were about 5dB higher than the left and right side. Furthermore, another factor which is important on the radiation pattern plots is that of the variation between the maximum and minimum E-field. By observing the traces on Figure 39, the E-field varied by about 12dB, 10dB and 10dB at 40km/h, 80km/h and 100km/h respectively. This finding indicates that 'blind' emissions spots can arise when only 2 viewing angles are observed around the vehicle during speed.

4.4 RF near-field probing (up to 300MHz)

Near-field scanning with RF probes was performed to locate components and areas on the vehicle which could contribute to the EMI. The output of the RF probe was connected through a 50 Ohm RF coaxial cable to the oscilloscope with its port set to a 50 Ohms to achieve impedance matching and the frequency content of the signal was analysed by observing the *voltage (dBuV)* and spectrum trace on the oscilloscope display.

The electric traction motors, incorporated within the rim of the rear wheels, were evaluated for their near-field emissions during speed to understand the critical frequencies that these might be generating. An electric probe was manually placed close to each electric traction motor on the rim of the rear wheels to detect RF emissions, as preliminary measurements with a magnetic field probe resulted in very weak voltage levels measured by the oscilloscope. The frequency response of the detected frequencies up to 300MHz, for each driving motor separately, is shown Figure 40 (a) and (b).

The traces indicated that the generated electric field levels from both motors (through the magnitude of the RF voltage) were particularly strong below 30 MHz. Above 30MHz, the left motor possessed broadband EMI which was spread between 120 MHz and 240 MHz and around 75 MHz for the right motor. Note that the interference close to the critical frequency of 75MHz, was also observed during the *far-field* frequency sweeps, for example Figures 17(b) and 18(b) and this could justify that this EMI could originated from the *right* motor. Near-field emissions can point to the cause of the RF emissions through the resemblance of such measurements with the corresponding far-field measurements. Figure 41 outlines this technique.

Figure 40: Near-field RF field emissions up to 300MHz during 45km/h constant speed (a) left and (b) right electric traction motor

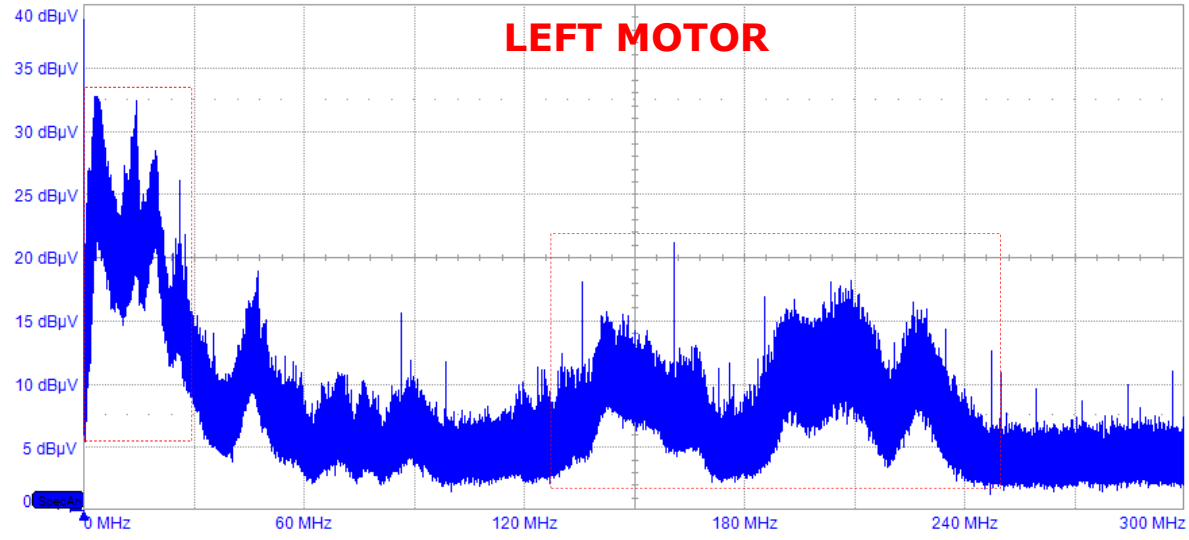

(a)

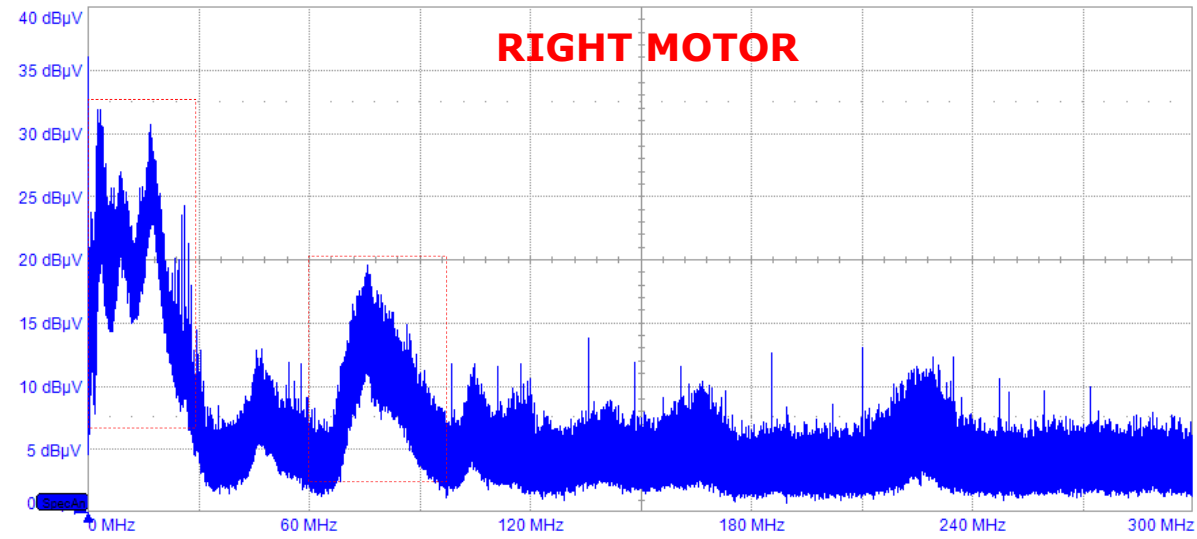

(b)

Figure 41: Assessing contribution of motor EMI during driving by examining the correlation (indicated by the dashed boxes) between near-field and far-field measurements (far-field 150kHz-30MHz: blue trace, far-field 30MHz-300MHz: red trace, near-field left motor: orange trace, near-field right motor: grey trace). Note the log-scale representation on the frequency axis to improve trace visibility towards the lower frequency bands.

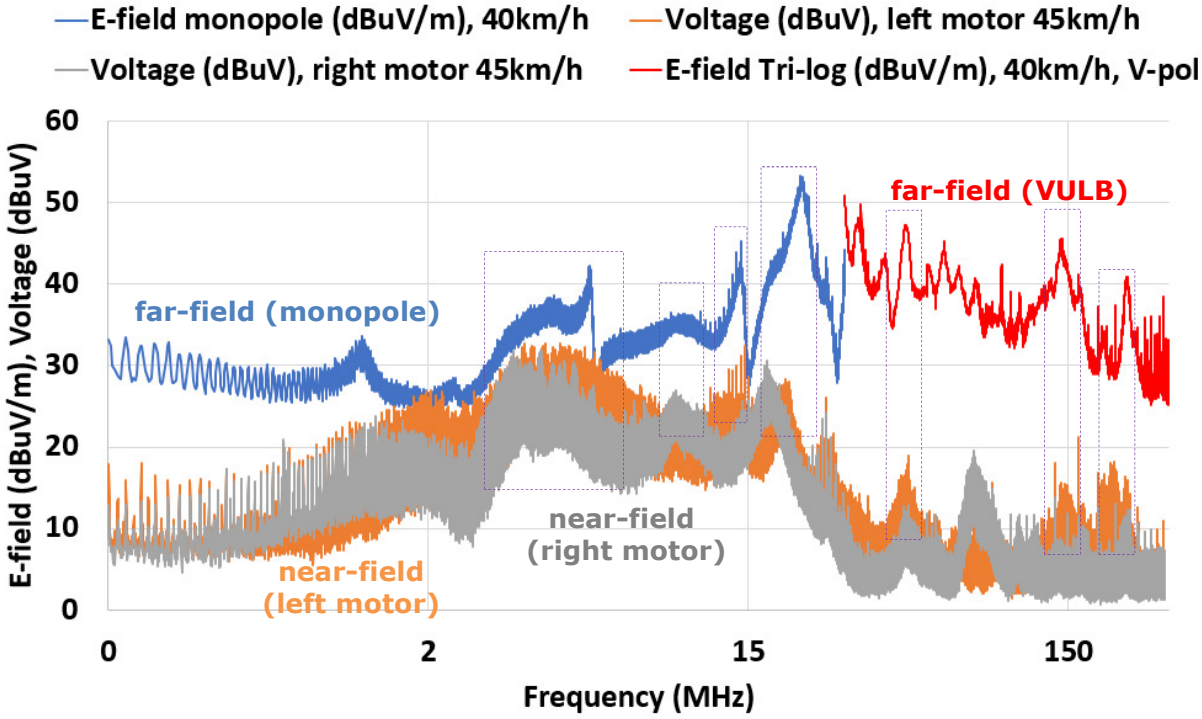

On Figure 41, the non-continuity on the *far-field* traces at 30 MHz is attributed to the different antenna type employed during the measurement (monopole for f<30MHz vs. tri-log for f>30MHz) and height above the metallic floor and does not constitute an error. A closer examination of the illustrated traces on Figure 41, in terms of frequency and amplitude content, shows that the EMI of the motor (grey and orange traces) has similarities (shown with the dashed boxes on the figure) at some frequencies with the far-field (blue and red traces) measurements. For example, the envelope of the trace of the far-field emissions around 5MHz (left and right motor), 14MHz (left motor) and 22MHz (left and right motor) possessed a good level of match with those of the near-field scans. A similar analogy applied for the frequencies around 75MHz, 150MHz (left motor) and 210MHz. Such a comparative approach could indicate that far-field EMI *at these frequencies* could be attributed to the operation of the electric traction motors.

Additional, near-field scans on the wires connected to the BUS module and the on-board driver's display are shown on Figure 42. A similar procedure, as carried out on Figure 41, can be applied to troubleshoot far field EMI by observing the spectrum of near-field scans. For example, the repetitive high frequency harmonics extending up to around 500MHz observed from the measurements on Section 4.1.1 could indicate that these originate from the on-board driver's display, as this has a very similar EMI behaviour shown by the response of the near-field scanning.

Annex 3, provides illustration of the positions used to evaluate the near-field emissions from the motors, the driver's display and the BUS module.

Figure 42: Near-field RF field emissions up to 300MHz
(a) BUS board and (b) on-board driver's display

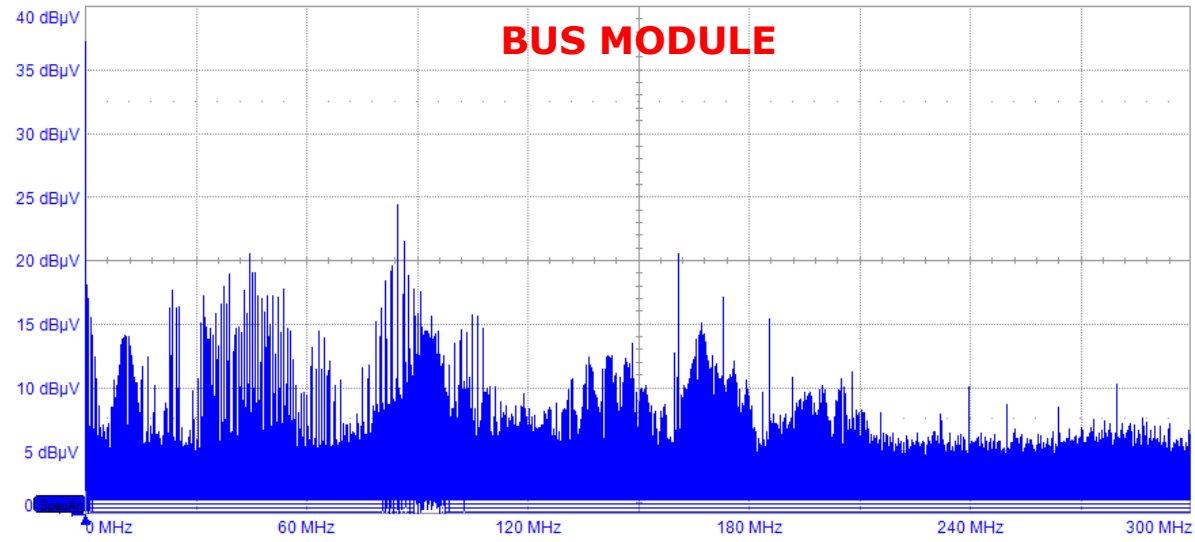

(a)

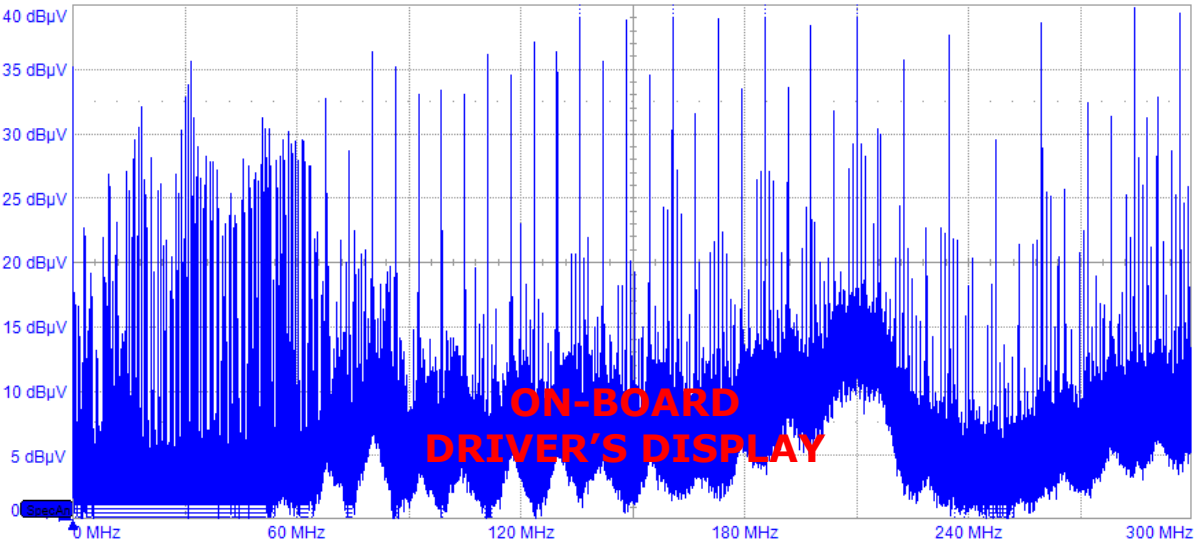

(b)

5 Conclusions

The electromagnetic emissions of a prototype solar-charged race-car were evaluated inside V*e*LA 9 validated automotive EMC semi-anechoic chamber of the European Commission's Joint Research Centre. The race-car was developed by the SolarCar Team of the Bochum University of Applied Sciences, Germany who were performing a research project about their vehicle.

The report outlined the test procedures applied during the measurements and the instrumentation equipment used for the execution of the EMC tests, based on CISPR 12 and IEC 61851-21-1 automotive standards. Measurements were carried out when the car was idle, whilst in driving mode and during charging to assess the levels of radiated and conducted emissions on the AC line.

Time domain measurements of the electric field and azimuth scans around the vehicle, beyond the legislative test methods prescribed on current automotive EMC standards (UNECE Reg.10 and CISPR 12), revealed that EM emissions under more dynamic and realistic driving conditions were strongly associated with the acceleration phase and speed of the vehicle and also depended on the observation angle around the vehicle. These findings fall outside the scope of the relevant automotive EMC standards, but it is important that these EM emissions are also considered in our interpretation for methodological clues, because the elevated EMI can affect vehicle components (aspect of susceptibility and functional safety).

Identification of the critical areas around the car responsible for the far-field radiation was assisted with azimuth scans performed by rotation of the turntable, while the vehicle was driven on the chassis dynamometer. Additional measurements with an electric monopole antenna, identified that radiated EM emissions were detected even below 30MHz, a frequency range which is not addressed on UNECE Regulation 10 and CISPR 12.

The vehicle was found to generate stronger EM fields during driving than when idle and the EMI was more pronounced in the vertical than in the horizontal antenna polarization. At the highest speeds, i.e. 80km/h and 100km/h, the vehicle generated emissions, which were particularly stronger, compared to the lower speeds, for the frequencies between 30MHz and 100MHz.

During charging, the conducted and radiated emissions exceeded the maximum allowed limit set by IEC 61851-21-1 for all charging scenarios, when charged with a charger supplied from the international component market an indication that it lacked dramatically proper RF filtering. High EMI was also identified on the radiated emissions during charging and radiation pattern plots identified that most of the generated electric field originated from the rear part of the vehicle, where the charger was installed.

Plots of radiation patterns at constant speed identified the critical angles of the emissions around the vehicle, which appeared to originate mainly from the rear side of the vehicle, where the electric motor, the power control modules and motor phase cables (for connecting the motor controllers to the wheel hub motors) were located.

Furthermore, near-field scans up to 300MHz were performed using an electric-field RF probe and this helped to reach the conclusion that some of the strong far-field emissions could be linked to the operation of the electric traction motor integrated within the rear wheel rims and the on-board driver's display.

Additional measurements were carried out with a vector network analyser (VNA) to evaluate the performance of the integrated Bluetooth antenna used for the wireless communication of the vehicle during outdoor race events. It was found that the VSWR response of the antenna was negatively affected by the closely spaced rear metallic registration plate of the car and appropriate adjustments were made to rectify this situation.

The exploratory EMC test methods developed on V*e*LA 9 of the EC's JRC, outlined on this report, for the assessment of the EMC profile of a vehicle can be utilised by an EMC test facility with applicability to any vehicle and recharging infrastructure and assist the identification and troubleshooting of potential sources of RF interference generated by an electrical or electronic system.

References

Armstrong K. “Including EMC in risk assessments”, 2010 IEEE International Symposium on Electromagnetic Compatibility, 2010, pp. 796 – 801

Chen, C., “Characterizing the generation & coupling mechanisms of electromagnetic interference noise from an electric vehicle traction drive up to microwave frequencies”, APEC 2000. Fifteenth Annual IEEE Applied Power Electronics Conference and Exposition (Cat. No.00CH37058), 2000, Volume: 2, pp. 1170 – 1176

CISPR 12 "Vehicles', motorboats' and spark-ignited engine-driven devices' radio disturbance characteristics - Limits and methods of measurement", fifth edition 2001 and Amd1: 2005.

Galassi M. Cristina, Nauwelaers P, Scholz H, Electro-magnetic compatibility of e-vehicles, , European Commission, Technical Report, 2015

IEC 61851-21-1:2017 Electric vehicle conductive charging system - Part 21-1: Electric vehicle on-board charger EMC requirements for conductive connection to an AC/DC supply

IEC 61851-21-2:2018 Electric vehicle conductive charging system - Part 21-2: Electric vehicle requirements for conductive connection to an AC/DC supply - EMC requirements for off board electric vehicle charging systems

Midya Surajit, Rajeev Thottappillil, “An overview of electromagnetic compatibility challenges in European Rail Traffic Management System”, ELSEVIER, Transportation Research Part C: Emerging Technologies, Volume 16, Issue 5, October 2008, Pages 515-534

Mutoh N, Nakanishi M, Kanesaki M. and Nakashima J, "EMI noise control methods suitable for electric vehicle drive systems," in IEEE Transactions on Electromagnetic Compatibility, vol. 47, no. 4, pp. 930-937, Nov. 2005. doi: 10.1109/TEMC.2005.857893

Ott, H. “Electromagnetic Compatibility Engineering”, Wiley Publishing, 2009

Pliakostathis-1, K, Zanni M, Trentadue G, Scholz, H, "Vehicle Electromagnetic Emissions: Challenges and Considerations," 2019 International Symposium on Electromagnetic Compatibility - EMC EUROPE, Barcelona, Spain, 2019, pp. 1106-1111. doi: 10.1109/EMC Europe.2019.8871957

Pliakostathis-2, K., Zanni M., Scholz H., Trentadue G., Assessment and analysis of the electromagnetic profile of prototype high-power-charging units for electric vehicles: Contribution to IEC 61851-21-2: Radiated and conducted emissions, radiated immunity and exploratory research, EUR 29704 EN, Publications Office of the European Union, Luxembourg, 2019, ISBN 978-92-76-01440-9, doi:10.2760/08750, JRC114312.

Shall H, Kadi M. "Study of the radiated emissions of an electric vehicle battery charger during the charge cycle," 2015 IEEE 12th International Multi-Conference on Systems, Signals & Devices (SSD15), Mahdia, 2015, pp. 1-5. doi: 10.1109/SSD.2015.7348148

Skibinski, G. L. Kerkman R. J. and Schlegel D, "EMI emissions of modern PWM AC drives," in IEEE Industry Applications Magazine, vol. 5, no. 6, pp. 47-80, Nov.-Dec. 1999. doi: 10.1109/2943.798337

UNECE Regulation 10, Revision 5 (9 October 2014), web link: https://www.unece.org/fileadmin/DAM/trans/main/wp29/wp29regs/2015/R010r5e.pdf (last accessed: 20 November 2019)

Williams T. “EMC for Product Designers”, 4th edition, Newnes 2007

Wisniewski, M, Kubichek R. ,Pierre, J. "EMI emissions up to 1 GHz from adjustable speed drives," IECON'01. 27th Annual Conference of the IEEE Industrial Electronics Society (Cat. No.37243), Denver, CO, USA, 2001, pp. 113-118 vol.1. doi: 10.1109/IECON.2001.976464

List of abbreviations and definitions

AC	Alternating Current
AF	Antenna Factor (dB/m)
Avg	Average (Detector)
BB	Broadband (emissions)
CW	Continuous Wave
DC	Direct Current
EC	European Commission
E-field	Electric field
EM	Electromagnetic
EMC	Electromagnetic Compatibility
EMI	Electromagnetic Interference
EUT	Equipment Under Test
H-pol	Horizontal Polarization
JRC	Joint Research Centre of the European Commission
L	Losses (dB) e.g. in coaxial cable
MT	Measurement Time
NB	Narrowband (emissions)
Pk	Peak (detector)
PWM	Pulse Width Modulation
QP	Quasi-peak (detector)
R	Voltage reading of the EMI receiver (dBuV)
RBW	Resolution bandwidth
RF	Radio Frequency
RFI	Radio Frequency Interference
SAC	Semi Anechoic Chamber
V*e*LA	Vehicle *Emissions* Laboratory
VNA	Vector Network Analyzer
V-pol	Vertical Polarization
VSWR	Voltage Standing Wave Ratio

List of figures

Figure 1: Illustrations of the receive antennas used for the measurement of the radiated emissions (a) Schwarzbeck VULB 9162 Tri-Log antenna, 30-8000 MHz and (b) active monopole E-field antenna ETS Lindgren 3301C, 30 Hz-50 MHz 7

Figure 2:The EMI test receiver used for the measurement of the radiated and conducted emissions 8

Figure 3: Line Impedance Stabilization Network (LISN) instrument used for the conducted emissions Rohde and Schwarz ENV4200, 150 kHz to 30 MHz, employing a transient limiter for the protection of the EMI receiver 9

Figure 4: Equipment used for near-field RF scanning of the vehicle (a) near-field electric and magnetic field probes by ETS-Lindgren, (b) oscilloscope Wavesurfer 510 by Teledyne LeCroy..... 9

Figure 5: Antenna and vehicle setup for the measurement of the radiated emissions inside VeLA 9 automotive EMC semi-anechoic chamber.....10

Figure 6: Radiated emissions (30-1000MHz), EV ON, 12V system (safe state), V-pol, (a) left, (b) right....12

Figure 7: Radiated emissions (30-1000MHz), EV ON, 12V system (safe state, parking light), V-pol (a) left and (b) right, H-pol (c) left and (d) right.....13

Figure 8: Radiated emissions (30-1000MHz), EV ON, 12V system (safe state, all lights ON), V-pol (a) left and (b) right, H-pol (c) left and (d) right.....13

Figure 9: Radiated emissions (30-1000MHz), EV ON, 12V system (safe state, brake, all lights ON), V-pol (a) left and (b) right, H-pol (c) left and (d) right 14

Figure 10: Radiated emissions (30-1000MHz), EV ON, 12V system (motor state, idle), V-pol (a) left and (b) right, H-pol (c) left and (d) right 15

Figure 11: Radiated emissions (30-1000MHz), 10km/h (cruise control), V-pol (a) left, (b) right, H-pol (c) left, (d) right 16

Figure 12: Radiated emissions (30-1000MHz), 20km/h (cruise control), V-pol (a) left, (b) right, H-pol (c) left, (d) right 16

Figure 13: Radiated emissions (30-1000MHz), 30km/h (cruise control) V-pol (a) left, (b) right 17

Figure 14: Radiated emissions (30-1000MHz), 40km/h (cruise control) V-pol (a) left, (b) right, H-pol, (c) left (note: one drive motor OFF), (d) right 17

Figure 15: Radiated emissions (30-1000MHz), 60km/h, V-pol (manual drive) (a) left, (b) right, H-pol (cruise control), (c) left, (d) right (note: one drive motor OFF).....18

Figure 16: Radiated emissions (30-1000MHz), 80km/h, V-pol (manual drive) (a) left, (b) right, H-pol (cruise control), (c) left, (d) right 19

Figure 17: Radiated emissions (30-1000MHz), 80km/h (cruise control) V-pol (a) left, (b) right 19

Figure 18: Radiated emissions (30-1000MHz), 100km/h, (cruise control) V-pol (a) left, (b) right, H-pol (c) left, (d) right 20

Figure 19: Conducted emissions (150kHz-30MHz), Trace 1=Phase, Trace 2=Neutral, Trace 6=noise floor, ONBOARD charger in series with DELPHI portable charger, (a) QP, (b) Avg. detectors 21

Figure 20: Conducted emissions (150kHz-30MHz), Trace 1=Phase, Trace 2=Neutral, Trace 6=noise floor, ONBOARD charger at I=16A, (a) QP, (b) Avg. detectors 21

Figure 21: Conducted emissions (150kHz-30MHz), Trace 1=Phase, Trace 2=Neutral, Trace 6=noise floor, ONBOARD charger at I=32A, (a) QP, (b) Avg. detectors.....21

Figure 22: Maximum radiated emissions (30-1000MHz) around the vehicle, EV ON, 12V system (safe state), (a) V-pol, (b) H-pol 22

Figure 23: Maximum radiated emissions (30-1000MHz) around the vehicle, EV ON, 12V system (safe state, parking light), (a) V-pol (b) H-pol 22

Figure 24: Maximum radiated emissions (30-1000MHz) around the vehicle, EV ON, 12V system (safe state, all lights ON), (a) V-pol (b) H-pol 23

Figure 25: Maximum radiated emissions (30-1000MHz) around the vehicle, EV ON, 12V system (safe state, brake, all lights ON), (a) V-pol (b) H-pol 23

Figure 26: Maximum radiated emissions (30-1000MHz) around the vehicle, EV ON, 12V system (motor state, idle), (a) V-pol (b) H-pol 23

Figure 27: Maximum radiated emissions (30-1000MHz) around the vehicle at 10km/h (a) V-pol, (b) H-pol 24

Figure 28: Maximum radiated emissions (30-1000MHz) around the vehicle at 20km/h (a) V-pol, (b) H-pol 24

Figure 29: Maximum radiated emissions (30-1000MHz) around the vehicle at 40km/h (a) V-pol, (b) H-pol 24

Figure 30: Maximum radiated emissions (30-1000MHz) around the vehicle at 60km/h (a) V-pol, (b) H-pol 25

Figure 31: Maximum radiated emissions (30-1000MHz) around the vehicle at 80km/h (a) V-pol, (b) H-pol 25

Figure 32: Maximum radiated emissions (30-1000MHz) around the vehicle at 100km/h (a) V-pol, (b) H-pol 25

Figure 33: Maximum radiated emissions (150kHz – 30MHz) around the vehicle at 40km/h (manual driving) 26

Figure 34: Electric field (radiated emissions) variation in time with vehicle's driving state up to 80km/h (aggressive acceleration), right side, V-pol 27

Figure 35: Electric field variation in time with vehicle's driving state up to vehicle's maximum speed (≈90km/h), right side, V-pol 27

Figure 36: Electric field variation in time with vehicle's driving state up to vehicle's maximum speed (≈90km/h), left side, V-pol 28

Figure 37: Electric field emissions from the vehicle during charging (32A) (a) V-pol, (b) H-pol [Traces: 1.Front, 2.Left, 3.Rear, 4.Right] 29

Figure 38: E-field (dBuV/m, QP detector) azimuth plot around the vehicle during charging (32A) at different frequencies [the equation used to calculate the IEC 61851-21-1 limit for each frequency with the QP detector was defined on Section 2] 30

Figure 39: E-field (dBuV/m, peak detector) azimuth plot around the vehicle at different constant speeds and frequencies [the equation used to calculate CISPR 12 limit for each frequency with the Peak detector was defined on Section 2] 31

Figure 40: Near-field RF field emissions up to 300MHz during 45km/h constant speed (a) left and (b) right electric traction motor 32

Figure 41: Assessing contribution of motor EMI during driving by examining the correlation (indicated by the dashed boxes) between near-field and far-field measurements (far-field 150kHz-30MHz: blue trace, far-field 30MHz-300MHz: red trace, near-field left motor: orange trace, near-field right motor: grey trace). Note the log-scale representation on the frequency axis to improve trace visibility towards the lower frequency bands. 33

Figure 42: Near-field RF field emissions up to 300MHz (a) BUS board and (b) on-board driver's display 34

Figure 43: Solar car setup fixed with non-conductive straps on the roller bench inside VeLA 9 automotive EMC semi-anechoic chamber 44

Figure 44: Setup and wire connections for testing the AC conducted emissions with a LISN during charging 45

Figure 45: Near-field scan measurements of (a) the electric traction motor (integrated within the rim of the wheel) (b) vehicle's BUS module and (c) on-board driver's display, using RF probe and oscilloscope 45
Figure 46: EMC tests monitoring, real-time trace analysis and data logging inside VeLA 9 control room 47

List of tables

Table 1: CISPR 12 peak detector limits for 10m antenna distance for assessing the radiated emissions from the vehicle 5

Table 2: Maximum allowed radio frequency conducted disturbances on AC power lines for on-board vehicle chargers 6

Table 3: Maximum allowed vehicle high-frequency radiated disturbances 6

Table 4: Configuration of the scanning receiver during the radiated and conducted emissions (NA: Not Applied) 9

Table 5: Test equipment for the radiated emissions measurements 42

Table 6: Test equipment for the conducted emissions measurements 42

Table 7: EMC test summary 43

Table 8: Vehicle specifications 48

Annexes

Annex 1. EMC laboratory equipment and instruments

Table 5: Test equipment for the radiated emissions measurements

Equipment description	Manufacturer	Model
Tri-log antenna	SCHWARZBECK	VULB 9162 (30MHz-8GHz)
EMI Test Receiver	Rohde and Schwarz	ESR7 (10Hz-7GHz)
Coaxial cables (with N-type connectors)	SSB Electronics	ECOFLEX 10
Active monopole rod antenna (for exploratory tests)	ETS-Lindgren	3301C (30Hz-50MHz)

Table 6: Test equipment for the conducted emissions measurements

Equipment description	Manufacturer	Model
LISN (Line Impedance Stabilisation Network)	Rohde and Schwarz	ENV 4200 (3-phase+N)
EMI (Electromagnetic Interference) Test Receiver	Rohde and Schwarz	ESR7 (10Hz-7GHz)
Coaxial cables (with N-type connectors)	SSB Electronics	ECOFLEX 10

Annex 2. EMC test summary

Table 7: EMC test summary

EMC test procedure			
Method	1) CISPR 12:2007 2) IEC 61851-21-1:2017		
Type of test	1) Radiated Emissions (static and dynamic driving) 2) High-Frequency AC Conducted Disturbances (charging) vs. grid		
Limit	1) Figure 2, CISPR 12:2007 2) Table 4 and 7, IEC 61851-21-1:2017		
Equipment Under Test			
EUT	1) Prototype Solar EV race-car 2) On-board EV battery charger		
State of EUT	Electric powertrain		
Test Laboratory			
Laboratory	V*e*LA 9 EMC SAC of EC's Joint Research Centre (Ispra, IT)		
Env. Conditions	Temperature: 23°C ±3 °C, Relative Humidity 50%		
Test Work Started	17/06/2019	Test Work Completed	21/06/2019

Annex 3. Supplementary laboratory illustrations

Figure 43: Solar car setup fixed with non-conductive straps on the roller bench inside VeLA 9 automotive EMC semi-anechoic chamber

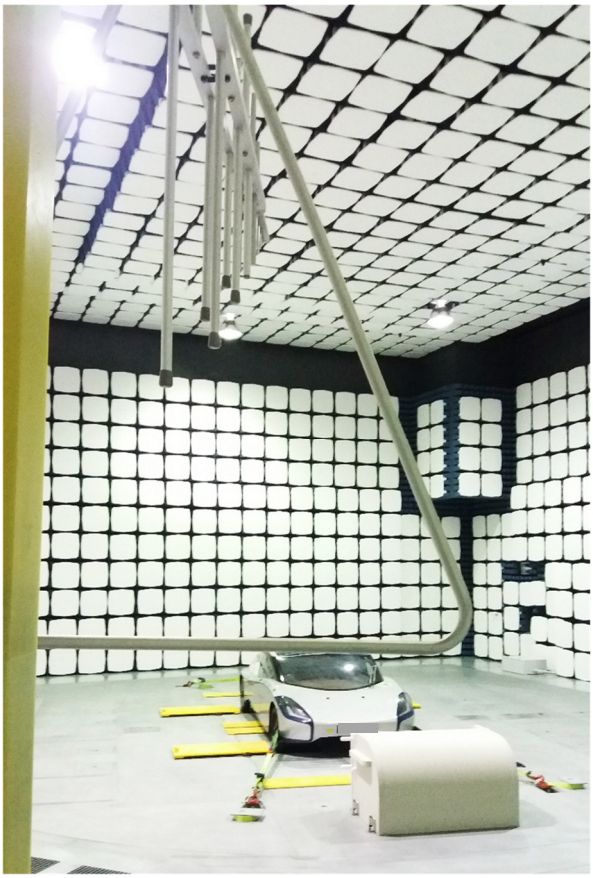

Figure 44: Setup and wire connections for testing the AC conducted emissions with a LISN during charging

Figure 45: Near-field scan measurements of (a) the electric traction motor (integrated within the rim of the wheel) (b) vehicle's BUS module and (c) on-board driver's display, using RF probe and oscilloscope

(a)

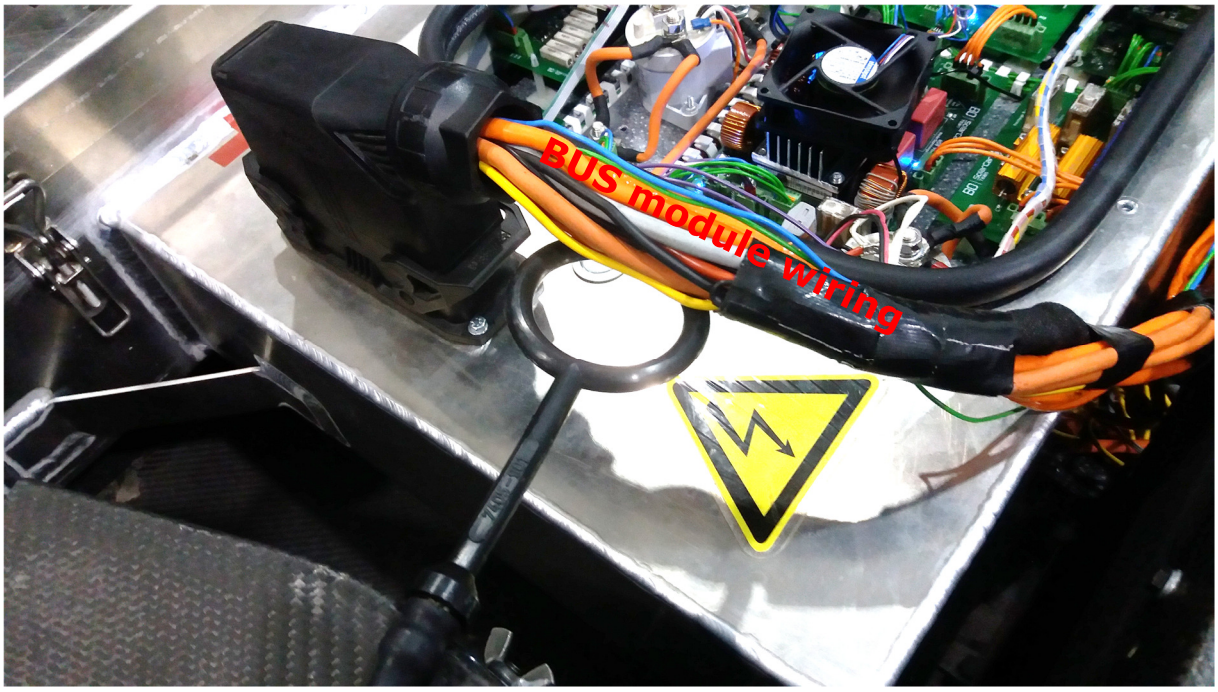
BUS module wiring

(b)

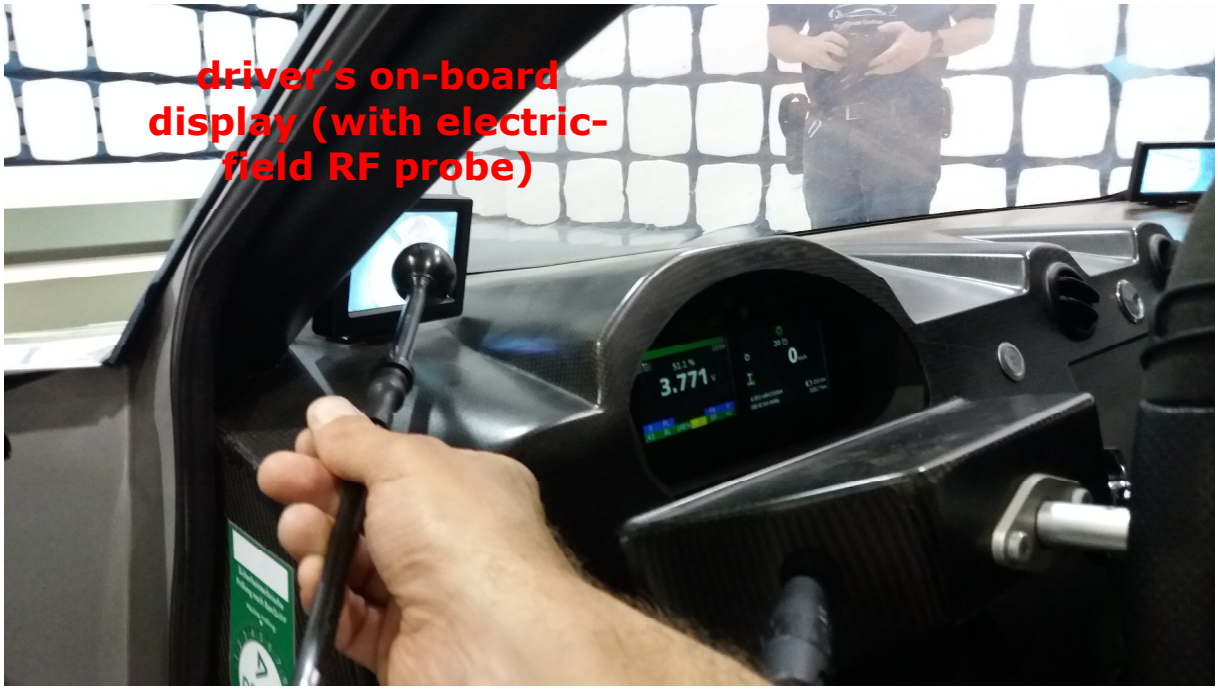
driver's on-board
display (with electric-
field RF probe)

(c)

Figure 46: EMC tests monitoring, real-time trace analysis and data logging inside VeLA 9 control room

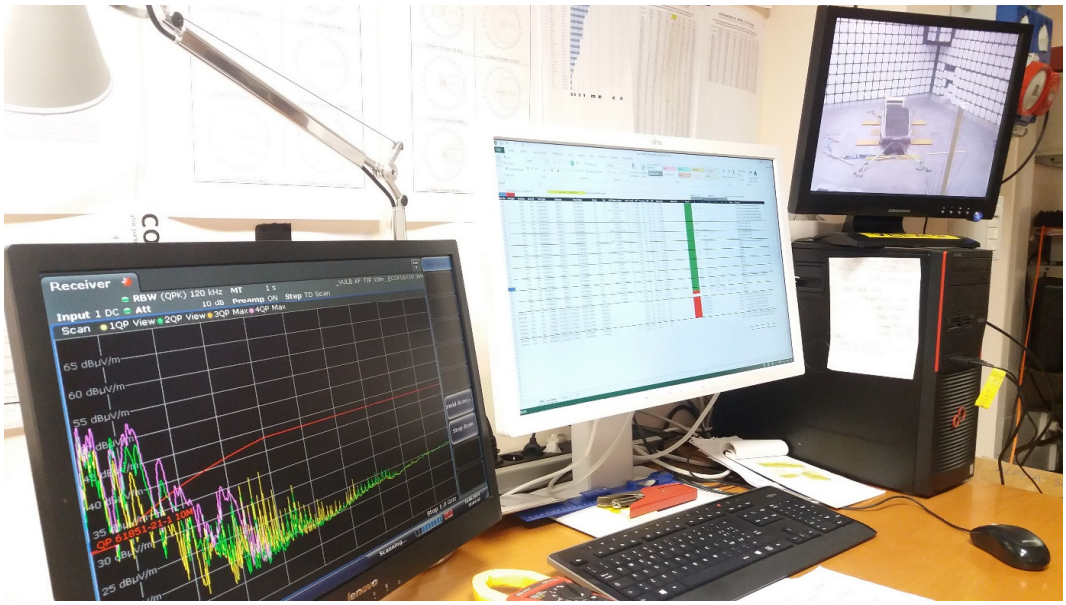

Annex 4. ThyssenKrupp SunRiser vehicle specifications

Table 8: Vehicle specifications

Length	4400 mm
Width	1760 mm
Height	1180 mm
Vehicle front-area	1.71m^2
Drag-coefficient	0.137
Weight	480kg
Maximum Speed	125km/h
Solar panel specifications	Area: 3m^2
	Maximum output power: 870W
	Gallium arsenide solar cells
Traction battery specifications	3350mAh (41kW/h total capacity)
	Chemistry: Li-ion cells
	90Vdc (discharged) 151.2Vdc(fully charged)
Motor	Max. Power: 15kW (total 2 motors)
Motor controller	175V, 122A

Blank page left intentionally

GETTING IN TOUCH WITH THE EU

In person

All over the European Union there are hundreds of Europe Direct information centres. You can find the address of the centre nearest you at: https://europa.eu/european-union/contact_en

On the phone or by email

Europe Direct is a service that answers your questions about the European Union. You can contact this service:

- by freephone: 00 800 6 7 8 9 10 11 (certain operators may charge for these calls),

- at the following standard number: +32 22999696, or

- by electronic mail via: https://europa.eu/european-union/contact_en

FINDING INFORMATION ABOUT THE EU

Online

Information about the European Union in all the official languages of the EU is available on the Europa website at: https://europa.eu/european-union/index_en

EU publications
You can download or order free and priced EU publications from EU Bookshop at: https://publications.europa.eu/en/publications. Multiple copies of free publications may be obtained by contacting Europe Direct or your local information centre (see https://europa.eu/european-union/contact_en).

KJ-NA-29991-EN-N

The European Commission's science and knowledge service

Joint Research Centre

JRC Mission

As the science and knowledge service of the European Commission, the Joint Research Centre's mission is to support EU policies with independent evidence throughout the whole policy cycle.

EU Science Hub

ec.europa.eu/jrc

@EU_ScienceHub

EU Science Hub - Joint Research Centre

EU Science, Research and Innovation

EU Science Hub

Publications Office of the European Union

doi:10.2760/800123

ISBN 978-92-76-13879-2